Technical Report
TR-17-12
February 2018

Revisiting bentonite erosion understanding and modelling based on the BELBaR project findings

Ivars Neretnieks
Luis Moreno

SVENSK KÄRNBRÄNSLEHANTERING AB

SWEDISH NUCLEAR FUEL
AND WASTE MANAGEMENT CO

Box 3091, SE-169 03 Solna
Phone +46 8 459 84 00
skb.se

SVENSK KÄRNBRÄNSLEHANTERING

ISSN 1404-0344
SKB TR-17-12
ID 1603464
February 2018

Revisiting bentonite erosion understanding and modelling based on the BELBaR project findings

Ivars Neretnieks, Luis Moreno
Royal Institute of Technology, KTH

Summary

In the 4-year BELBaR project considerable amounts of new information has been generated concerning bentonite erosion in fractured crystalline rocks. Earlier known mechanisms and processes have found additional support. Floc formation has been shown to influence erosion rates under flowing conditions and has also been found to cause erosion in sloping fractures due to sedimentation of the flocs. These mechanisms have now been incorporated in the quantitative models for erosion simulations. The underlying mechanisms for stack formation of smectite sheets caused by divalent ions such as calcium have been confirmed by density functional theory, DFT, modelling. This additionally confirms the earlier observations and models used to describe the behaviour of montmorillonite in waters with mixtures of different ions.

A large number of erosion experiments with clays with the naturally present accessory minerals have shown that these rapidly clog filters and variable aperture fractures of the sizes expected in fractured granite. This slows down erosion flux by 2–3 orders of magnitude, or more, compared to the rates in clays purified from the accessory minerals on which the present model has been built. The present model is described in detail in Neretnieks et al. (2016a). In addition to the experiments on which the model is based some benchmark experiments in the BELBaR project were now used for additional validation.

The eroded montmorillonite forms flocs that sediment in sloping fractures. This is accounted for in the model. The rate of transport of the flocs is modelled as a flow of an agglomerate fluid with a viscosity like water. Experiments from the BELBaR project and information in literature suggest that the sedimenting agglomerate fluid becomes so much more viscous with time that it may slow down the erosion because of fracture clogging by a gel-like sediment.

In large aperture sloping fractures that are not rapidly clogged the sedimenting clay will collect at the bottom of the fracture. Intersecting fractures can allow the sediment to migrate further into the fracture network when the next fracture has a slope steeper than the angle of repose (friction angle). For the accessory minerals this is expected to be on the order 25–45°, whereas it can be lower for the smectite agglomerates. This suggests that there is a distinct possibility that the accessory minerals will fill the fracture network below the tunnel and/or deposition hole after some initial loss of clay and stop further erosion. These effects can be of special importance for KBS-3H drifts. The effects of the accessory minerals are not included in the present model. Specially designed experiments with clays with and without accessory minerals could be made to explore this further. It may also be possible to support such clogging of fractures by modelling.

The main weaknesses in the present model are that

- The viscosity of the sedimenting agglomerate fluid is probably seriously underestimated as the effect of aging is not accounted for.
- The potential clogging of fractures by accessory minerals is not accounted for.

There is a potential that both these effects independently may decrease the erosive loss by several orders of magnitude.

No information has been found in the BELBaR investigations or in other relevant literature on montmorillonite suspension properties and behaviour that could seriously increase the erosion rate above that of the model of Neretnieks et al. (2016a).

Sammanfattning

I det fyraåriga BELBaR projektet har mycket ny information tagits fram om bentoniterosion i sprickigt kristallint berg. Tidigare kända processer och mekanismer har fått ytterligare stöd. Flockbildning har visats ha stor betydelse för erosion i sprickor med strömmande vatten och också visat sig ge upphov till erosion i lutande sprickor genom sedimentation av flockarna. Dessa mekanismer har nu infogats i den kvantitativa modellen som används för att simulera erosion. De grundläggande orsakerna till att montmorillonitpartiklarna bildar täta stackar i vatten med tvåvärda katjoner, som kalcium har visats med hjälp av täthetsfunktionalteori, DFT. Detta stärker ytterligare de observationer och modeller som används för att bestämma montmorillonits uppförande i vatten med blandningar av olika joner.

Ett betydande antal erosionsexperiment med leror i vilka de naturligt förekommande accessoriska mineralen inte tagits bort visar att dessa snart sätter igen filter och de tunna sprickor som förväntas i sprickigt kristallint berg. Detta minskar erosionen med 2 till 3 storleksordningar jämför med försök där de accessoriska mineralen tagits bort. Den använda modellen baseras på försök med ren montmorillonit renad från accessoriska mineral. Modellen beskrivs i detalj i Neretnieks et al. (2016a). Förutom de experiment som modellen byggdes på har den nu ytterligare verifierats med de ”benchmark” experiment som gjordes i BELBaR projektet.

De eroderade montmorillonitpartiklarna bildar flockar som sedimenterar i lutande sprickor. Modellen tar nu hänsyn till detta. Flockflödet beskrivs med en modell som beskriver flocksuspensionen som en vätska med viskositet som vatten. Experiment i BELBaR och från litteraturen tyder på att denna vätskas viskositet ökar med tiden så mycket att den inte kan transporters bort så snabbt som nya unga flockar kan bildas och att sprickor skulle kunna sättas igen av en åldrad flockvätska.

I lutande sprickor med stor apertur som inte snabbt sätts igen av flockvätskan sedimenterar leran som innehåller accessoriska mineral till botten av sprickan och ansamlas där om den inte kan rinna vidare nedåt i en annan lutande spricka i spricknätverket. En sådan spricka måste ha en större lutning än rasvinkeln för leran. Rasvinkeln för accessoriska mineral förväntas vara 25–45° men är lägre hos sediment som inte innehåller accessoriska mineral. Detta tyder på att de accessoriska mineralen så småningom borde kunna fylla spricknätverket under tunnel och depositionshål och hindra fortsatt erosion. Detta skulle kunna ha särskilt stor betydelse för KBS-3H tunnlar. Denna tänkbara effekt av de accessoriska mineralen är inte inkluderad i erosionsmodellen. Det borde vara möjligt att göra experiment med leror med och utan accessoriska mineral för att utforska detta ytterligare. Det är också möjligt att utveckla modeller för att studera detta.

De främsta svagheterna i den befintliga modellen är att:

- Viskositeten hos flockvätskan är sannolikt mycket underskattad eftersom effekter av åldring inte har beaktats.
- Den potentiella igensättningen av sprickorna med accessoriska mineral har inte beaktats och kvantifierats.

Det finns en potential att båda dessa effekter oberoende av varandra skulle kunna minska erosionsförluster med många storleksordningar.

Vi har inte funnit någon information i BELBaR resultaten eller i andra källor relevanta för montmorillonitsuspensioners egenskaper och uppförande som nämnvärt skulle kunna öka erosion över vad modellen i Neretnieks et al. (2016a) förutspår.

Contents

1 Background

It is assumed that the reader is rather familiar with nuclide waste repository concepts in fractured crystalline rocks where bentonite clay is used as buffer and backfill.

Bentonite clay will be used to embed radioactive waste canisters in deep geologic repositories at large depths in water saturated crystalline rocks (SKB 2011, Posiva 2012). The compacted swelling bentonite protects the canisters from rock movement and from direct exposure to groundwater seeping in the fractures in the rock. It also decreases microbial activity near the canister surface. It delays influx of corrosive agents to the canisters and, should a canister be breached, it delays the release of nuclides from the damaged canister. One of the main concerns for the integrity of a repository is that some bentonite due to its strong swelling pressure will be lost by intrusion into the fractures and be carried away by the seeping water as sol. This can happen when the salt concentration in the water is low and the water composition becomes favourable for sol formation. Key issues are the *rate of bentonite intrusion into fractures*, conditions for and rate of *solubilisation* of the smectite in the clay and *rate of transport* of the released colloids.

In the BELBaR project a considerable number of experiments were made in which bentonite clay was allowed to intrude a fracture with either stagnant water or slowly seeping water. The intrusion of the clay into artificial fractures and the release of smectite into the water in the fractures were studied. An important aim of these experiments was to obtain data that could be used to develop models that can be used to assess the loss rate of bentonite from deposition holes and tunnels hosting radioactive waste canisters. In addition a number of experiments were made to study the underlying mechanisms for bentonite swelling and smectite solubilisation. Previously derived conceptual, mathematical and numerical models were refined and modified based on the experimental results.

The vast amount of information gathered during the four-year project has been reported in a number of reports, deliverables, and in publications in journals. Not all this information and experimental results could be fully digested by the participants during the final phases of the project. Now the reporting is finished and this can be done. The main results related to bentonite erosion are found in a number reports, the BELBaR deliverables, D2.2 (Neretnieks et al. 2013), D4.10 (Liu et al. 2015), D4.11 (Missana et al. 2016), and D5.3 (Neretnieks et al. 2016b).[1]

[1] http://www.igdtp.eu/index.php/european-projects/belbar

2 Aims and scope

The objective and scope defined by SKB for the present report is stated as follows.

“The first step in this project is an evaluation of how well the current model matches the experimental data from the BELBaR project. The assignment is to:

- Collect and compile available data, mainly from the BELBaR project but possibly also from other sources, to be able to use them for model testing.
- Verify the model against experimental data from the BELBaR project.
- Identify weaknesses in current models using experimental information from the BELBaR project.
- Identify the needs for additional experimental data.
- Documentation.”

We approach these aims in the following way. The present report makes an effort to further scrutinise the information that is relevant for the predictive modelling of bentonite loss from deposition holes and tunnels, to find support for the model(s) and also, which is as important, to find and point out any contradictory evidence in the model(s). This is primarily done by revisiting the experiments to see how these affect the conceptual, mathematical and numerical model(s) that can be used to simulate and predict clay expansion and erosion. Important issues such as influence of divalent ions, mainly calcium, rheologic properties of clay paste and gel, gel structure and agglomeration and ion composition of water are discussed mainly as they affect the models. In addition the transport and fate of the eroded clay is addressed to explore if it could influence the erosion rate. The report does not discuss radionuclide transport with released colloids.

3 Short summary of main components of the model concept

Gel denotes clay that forms cohesive structures where the repulsive forces just balance the attractive forces between the particles that make up the clay. This avoids the often-used term “repulsive gel”. A gel with a given volume fraction of clay particles can form in pore water with ion concentrations above the critical coagulation concentration, CCC. *Sol* denotes a dilute suspension of colloidal size particles that do not agglomerate because repulsive forces between particles keep them apart. The ion concentration must be below the CCC. *Paste* describes clay that could take up more water and expand until it either can become a coherent gel or could expand further and release particles into a sol. This is in agreement with Hedström et al. (2016). By *agglomerate* and *floc* we mean that clay particles are loosely arranged in complex flexible structures in water below CCC conditions. The difference between floc and gel is not quite clear at present but we try to separate the terms because there are indications that the attractive forces in gel and floc are different and the two behave differently when subject to stress.

One of the key questions in the BELBaR project and in earlier similar projects is under what conditions and at which rates smectite rich clays can solubilise and release colloidal smectite particles to water. The concept of a critical coagulation concentration CCC is old and is commonly used to assess solubilisation conditions. In water compositions above CCC clay will form a gel when it has expanded to an equilibrium volume fraction of smectite. No particles can be released spontaneously to water, stagnant or flowing. Below the CCC colloidal particles are spontaneously released to water and can be carried away by seeping water. Only recently it has been shown that the CCC concept as commonly used can be (strongly) misleading because not only the ionic composition of the counterions in the bulk water in contact with the clay determines if sol can form. Also the type of ions and the ion composition in the clay are important. The cations attached to the charged smectite clay particles can be exchanged with those in the water and entirely change the gel/sol conditions (Hedström et al. 2016). Nevertheless the simple *concept* is useful for the typical conditions and clays of interest. In clays with much sodium in ion exchange positions coming in contact with less than 5–10 mM of sodium rich groundwaters solubilisation may occur. This is not the case for calcium-dominated clays where more than 80–90 % of the charge compensated ions are divalent (calcium and magnesium). Then no solubilisation occurs under expected flowrate conditions and for water compositions down to pure water. However, it is recognised that, given time, seeping water with essentially only sodium, by ion exchange, could decrease the calcium content in the clay.

Much of the research in BELBaR has been focused on conditions when solubilisation can occur. In this report we mostly discuss models and experiments when this is fulfilled because observations clearly show that in waters with ion concentrations higher than about 10 mM of relevant ions, Na and small amounts of K, Ca and Mg, erosion of colloidal matter is very small, irrespective of flowrates in the ranges expected under repository conditions. Flow velocities less than 10^{-4} m/s are considered. Under those conditions a coherent gel forms that does not readily release colloidal particles. Nevertheless also strongly calcium-dominated clays can also expand into fractures and clay can be lost from the source. Such clays do not form cohesive gels. The smectite sheets aggregate in stacks. In sloping fractures the stacks can detach from the bulk of the clay and sediment.

At lower concentrations than about 5–10 mM NaCl detachment of smectite flocs and large agglomerate sheets can take place. Smectite expansion, release and sol formation in water is quite well understood in systems dominated by monovalent ions, such as sodium, which is the dominating cat-ion in the dilute groundwaters at Forsmark (Laaksoharju et al. 2008). However, the waters also contain calcium, which also influences the smectite behaviour in important ways. The expansion and erosion are quantitatively modelled by the dynamic clay expansion and release model (Neretnieks et al. 2009). The model has a strong foundation in fundamental processes where the attraction and repulsion forces between particles resulting in expansion are balanced by the friction force of the particles moving in the water. This model has been validated by detailed experiments in stagnant water and covers smectite volume fractions from repository densities down to five orders of magnitude lower (Liu 2010, Liu et al. 2011).

At high compaction the smectite particles are present in stacks of parallel smectite sheets. Repulsion forces between sheets are dominated by the osmotic pressure described by the interacting diffuse double layers of dissolved ions close to the surfaces of the smectite sheets. At smectite volume fractions below about 1 % the particles become free to rotate. Their movement is caused by Brownian diffusion. This model and its use in prediction of expansion and erosion in fractures are described in Neretnieks et al. (2009) and references therein. In that modelling the dynamic clay expansion was also coupled to the simultaneous ion exchange between the expanding paste/sol and the water seeping in the fracture. One finding that was later useful to simplify modelling was that the exchangeable ion composition on particles near the paste/sol/water interface would rapidly equilibrate with the approaching water. As a consequence it was assumed that the approaching water composition would determine the conditions for sol formation. When the charge of the smectite particles is more than 80–90 % compensated by divalent ions such as Ca and Mg, such clay does not release colloidal particles even in deionised water. This has been experimentally verified and is understood to be caused by ion correlation effects (Guldbrand et al. 1984, Jellander et al. 1988, Jönsson et al. 2009, Yang and Liu 2015, Yang et al. 2016). In such clays the smectite sheets collapse into stacks with several tens of sheets. These effects have been modelled by density functional theory, DFT, and fully support the experimental findings (Liu 2013). The stacks repel each other and also calcium dominated clays swell, but the swelling is much more limited. The reason(s) for the stack repulsion and for the lack of sol formation is not well understood.

Within the above model concept in which the release of smectite particles is governed by diffusion of the particles from the paste/sol interface, the transport capacity of seeping water is readily obtained using a model where particles diffuse into water gradually building up a moving boundary layer of increasing extent, which when leaving the clay region carries with it the smectite particles. The model is more complicated than the conventional equivalent flowrate, Qeq-models with dissolved solutes (Neretnieks et al. 2010), by that the presence of colloids strongly influences the sol viscosity and thus the flow-field itself. This is mentioned here because many of the experiment in BELBaR did *not* confirm this viscosity impact. In those experiments it was found that after the smectite particles have been released at the paste/sol interface they rapidly agglomerate and form loose flocs in the seeping water. Floc formation was not included in the original dynamic model. The floc formation is interpreted to be due to the weak shear forces caused by the velocity gradient along and across the fracture with the seeping water. This causes the smectite particles to slowly rotate, each at a somewhat different rate. This allows the positively charged edges of the particles to come in contact with the negatively charged faces and form complex three-dimensional structures. This has been shown in studies by Hedström et al. (2016). The flocs can contain thousands of particles, which are only loosely held together. The flocs are flexible and can squeeze trough narrow passages and re-form afterwards (Jansson 2009, Neretnieks et al. 2009). A special characteristic of the flocs is that they readily flow with the seeping water without much influencing its velocity (Schatz et al. 2013). It seems that the water flowrate is not impeded by the presence of the flocs, which are carried away by the seeping water. This is in contrast to what would be the case if the smectite particles had not formed flocs. Then the sol would have had a considerably higher viscosity, which would slow down the fluid at the paste/sol interface and decrease the release rate.

By including floc formation and assuming that it is very rapid once colloidal smectite particles have been released from the clay, a considerably simpler model could be devised. This could be done at the expense of having to introduce one adjustable parameter, namely the volume fraction of smectite at which colloids are released at the paste/sol interface. That volume fraction was found to be around 1.5 % to obtain a good fit to a number of experiments at different flow velocities and ion concentrations (Neretnieks et al. 2016a). The preceding model without floc formation needs only parameters that can be/had been determined by independent experiments and were based on established physical and chemical processes and data.

When there is floc formation gravity can detach and pull the flocs, which are slightly denser than water downwards. Without floc formation the individual smectite particles are negligibly mobilised by gravity because of the very much larger surface to mass ratio.

In sloping fractures, the flocs are made to sediment at a pace that results in loss comparable to or larger than that observed and modelled by flow in horizontal fractures (Neretnieks et al. 2016a). Although floc formation and sedimentation had been observed and reported earlier (Neretnieks et al. 2009, Jansson 2009), its consequences and quantitative modelling was only addressed in BELBaR based on experiments in sloping fractures (Schatz et al. 2013, Schatz and Akhanoba 2016).

The extension of the model to also account for sedimentation of the flocs formed at the paste/sol interface describes the release and sedimentation velocity in two distinctly different ways depending of the aperture of the fractures. When the flocs first form and are released they are small compared to the aperture of the fracture and are modelled by Stokes law for individual sphere movement in a fluid. The small flocs have different sizes and the larger, faster flocs catch up with smaller, join them and form larger flocs, which increase their velocity etc. When a floc has grown in size to become as large as the fracture aperture, its further growth forces it to touch the walls. Wall friction then sets the pace for the coin or sheet-like floc movement. The settling velocity can then be estimated by the so-called "cubic law", which describes how a denser "liquid", the floc, sediments in a less dense liquid, the water. Of special interest is that the cubic law predicts that the floc velocity is proportional to the fracture aperture to the third power. In the experiments in 1 mm aperture and 0.1 mm aperture this was not found to be the case. The loss rate due to sedimentation was found to be proportional to the aperture and not to the third power. However, by inspection of the pictures of the floc movement it is found that in the larger aperture fracture the sedimentation seems to be in narrow streams, possibly string-of-pearl-like streams, whereas in the narrow fracture the flocs have formed large sheet-like regions that are in contact with the fracture walls. In the fracture with the larger aperture it seems that the release rate is set by the release rate of the initial flocs, the small "spheres", whereas in the narrow fracture the sliding velocity of the sheet-like floc(s) determines the overall transport rate as it will not allow new flocs to form before the previous flocs have moved away. Most real fractures at repository depth are expected to have mean apertures much smaller than 1 mm. It seems that the transition region between the two floc-migration mechanisms is in the aperture range 0.1 to 1 mm. This implies that in larger aperture fractures the mass loss rate will be proportional to the aperture, whereas in smaller apertures the mass loss will be proportional the aperture to the third power.

For fractures larger than 0.1 mm the total loss rate of smectite from clay expanding into a fracture is proportional to the size (radius times the aperture) of the expanded clay surrounding the deposition hole at any given time according to the model(s). This size in turn is set by a balance between the rate of expansion of the paste/gel from the deposition hole, the source, and the rate of loss at the paste/sol interface, the rim. The radius to the rim will grow due to the expansion from the source until it balances the rate of loss at the rim. The distance to the rim may even start to recede if the source is noticeably depleted. Then the extrusion rate decreases. This was found in most of the long-term laboratory experiments in which the source volume was small (Schatz et al. 2013). In a repository deposition hole this is not expected because of the very large mass of smectite present.

In summary: The model used to simulate loss of smectite from the deposition hole or drift has two main model components. The first is the dynamic clay expansion model that describes how compacted bentonite takes up more water, generates strong swelling pressure and swells into available space- the fractures. This model is valid for a wide range of ion concentrations in the pore water. For monovalent ions the swelling can be extensive. It is also valid for calcium-dominated clays up to the point where swelling pressure drops to zero, which occurs at volume fractions in the range of 10–20 %. It may be noted that clay is lost from the deposition hole by expansion into the fractures, even if there is no erosion at the rim.

The second model component is that which describes the loss at the rim. This can occur in stagnant water in the fracture by smectite floc sedimentation and in addition by seeping water that carries away the released smectite flocs and colloids Erosion by floc formation at the clay/water interface can only occur in waters with concentrations below 5–10 mM for some clays but can be on the order of 20 mM for other sodium dominated clays. The two model components must be solved simultaneously because they influence each other.

3.1 Some additional mechanisms that can limit clay loss

3.1.1 Accessory minerals

A potentially limiting mechanism is caused by formation of filters of accessory minerals in the fractures and inlets to the fractures by the considerable amount of accessory minerals present in bentonites. Natural bentonites contain accessory minerals in amounts of around 10 % or more. These minerals include quartz, feldspars, kaolinite and other non-swelling clays. These particles have a size distribution ranging from colloidal size up to a few tenths of a mm. On average they are very much larger than the smectite particles (Richards 2010). They have negligible inherent charge and do not form swelling structures. They are carried along by the swelling clay but left behind when the smectite sol forms and migrates away.

Predictions have been made that the accessory minerals in the bentonite will clog fractures by forming filters of the mineral particles when they were left behind in the fractures when smectite erodes and is carried away (Neretnieks et al. 2009). It was also shown that a mm or at most a few mm thick layer of mineral particles of sizes similar to the accessory minerals could essentially stop smectite particle passage (Richards 2010). Also the experiments with as-received MX-80 reported in Birgersson et al. (2009) with smectite penetrating stainless steel filters supports this idea.

To interpret the experiments by different research groups it is important to understand the different pre-treatment methods used. ClayTechnology and B+Tech use an elaborate method to prepare the clays for the experiments (Schatz et al. 2013). According to Karnland et al. (2006), the procedure removes all particles larger than 2 μm The resulting clay contains practically only smectite and negligible amounts of accessory minerals.

Ciemat use a simpler procedure, which retains the insoluble accessory minerals in the clay after homo-ionisation (Missana et al. 2011).

3.1.2 Fate of eroded material

The released accessory minerals and flocs in the seeping water must be carried away from the vicinity of the source to make room for more release. In the experiments in sloping fractures the sediments collect at the bottom of the “fracture” and build up heaps of sediments. In all pictures from experiments with as received clays, which contain accessory minerals the heaps have a slope between 25–45 degrees. This also is the case with strongly calcium-dominated clays (CaMt) without accessory minerals. In such clays the smectites particles form stacks of many tens of sheets that sediment. If the observed slope is the angle of repose (friction angle) it implies that in the next lower fracture intersected, the sediment cannot move on unless the slope is steeper than the angle of repose. Eventually a fracture with smaller angle would be encountered. Depending on the properties of the fracture (channel) network the sediment could build up to the source (deposition hole or drift). Erosion would then stop. In some experiments with clays without accessory minerals the slope of the sediment is much smaller and could be close to zero. The agglomerate fluid, AF, consisting of the flocs would flow nearly as a liquid and could move away also horizontally in the network to large distances.

Figure 3-1 gives an illustration of the fate of eroded material in a sloping fracture.

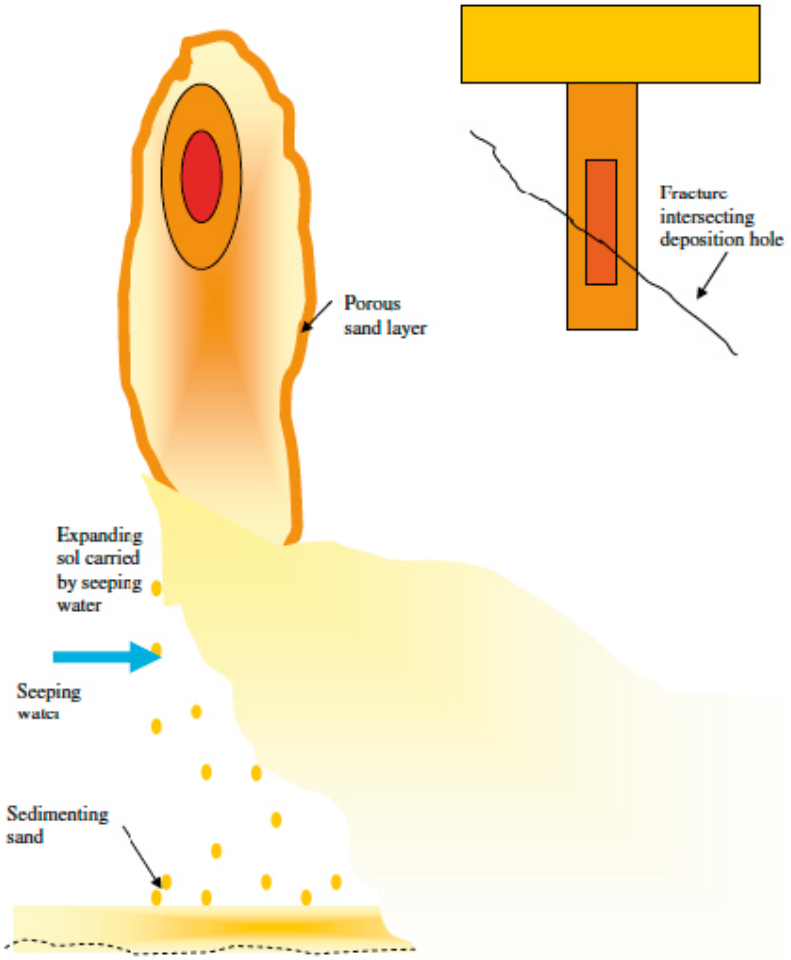

Figure 3-1. *Illustration of how a sand (accessory mineral) region could develop in a fracture around a deposition hole or drift. The sand can be breached and sediment to the bottom of the fracture (Neretnieks et al. 2009)*

4 Erosion experiments and their modelling

4.1 Artificial fractures

4.1.1 B+Tech

At B+Tech a number of erosion experiments have been performed with different bentonites and different waters under no-flow as well as under flow conditions in horizontal fractures with 1 mm aperture (Schatz et al. 2013). The clays used were MX-80 as received, called WyBt, and homo-ionic NaMt and CaMt and 50/50 mixtures of the two latter. These clays contained practically no accessory minerals. Thirteen tests were made where measurements followed the clay expansion and erosion over time. The artificial fracture was 26×26 cm and the compacted bentonite plug was 2 cm in diameter and 2 cm high compacted to a dry density of 1.59 g/cm^3.

Photographs and measurements of mean radius of extruded clay and eroded mass found in the effluent water were made. After the tests with durations running from around 500–700 hours and some very long tests up to 2688 hours, the remaining mass in the source, the extruded mass in the fracture as well as other remaining sedimented mass was determined gravimetrically.

The experiments confirmed previous observations and theoretical predictions that at ionic strengths above 5–10 mM practically no erosion took place in any of the clays and clay mixtures in 1 mm aperture fractures. Under no-flow conditions in one test the clay expanded into the fracture with a decreasing rate over time, but was still expanding after 700 hours, having expanded 27 mm during this time. This agrees well with the predictions by the dynamic clay expansion model (Neretnieks et al. 2016a, Appendix 2).

Clays with and without accessory minerals expanded several cm into the 1 mm aperture fractures under no-flow as well as under flow conditions. The largest erosion rates were observed in deionised water. The observed erosion rates were considerably lower than those predicted by Liu et al. (2011) model for smectite behaviour as implemented in the numerical code (Moreno et al. 2010, 2011). The numerical solution technique had at that time been found to give inaccurate result unless in practice prohibitively fine discretisation was used. A more efficient and faster code was developed, which, however, also considerably overestimated the erosion rates (Neretnieks et al. 2016a). Examination of details in the photographs of the expanding clays under flow conditions revealed that smectite particles in the sol agglomerated to form flocs just after the sol particles were released from the paste/sol interface. The flocs were carried away by the seeping water, seemingly with the same velocity as the seeping water without flocs. Incorporating floc formation and floc transport in the model gave quite good fits. However, it must be noted that in this case one parameter, namely the volume fraction of smectite particles at the paste/sol interface, at which sol and then flocs form, had to be used as a fitting parameter. This volume fraction was found to be 1.5 %, which seems to be a reasonable value, considering that in the model without floc formation it is predicted that at the paste/sol interface the volume fraction should be between 0.5 to 1 % depending on water composition and flow velocity. The latter prediction is based on the physics and chemistry underlying the dynamic clay expansion model and uses no adjustable parameters.

With the modified and now simple model the agreement with the experimental erosion rates was quite good as is shown in Figure 4-1. The water velocity spans 5.6×10^{-6} to 1×10^{-4} m/s. More details of this modelling are given in Neretnieks et al. (2016a, Appendix 2).

The above-described experiments were performed in horizontal fractures. The smectite mass in the flocs remaining in the fractures at the end of the experiment was assessed by collecting the "retained mass". In these experiments it was also found, by dye injection, that the water containing the flocs seemed to flow with the same velocity as the floc free water. This suggests that the presence of freshly formed flocs has a minor influence on the viscosity of the floc slurry.

One of the main findings of the erosion experiments in flowing fractures was that there was no erosion of NaMt in water with more than 8.6 mM NaCl. This supports the model predictions that above about 10 mM the erosion rate should decrease very much. Another interesting observation at the lower ion concentrations is that the 50/50 mix of NaMt and CaMt erode about 3 times slower and the as-received MX-80 bentonite erodes about 10 times slower than the pure NaMt.

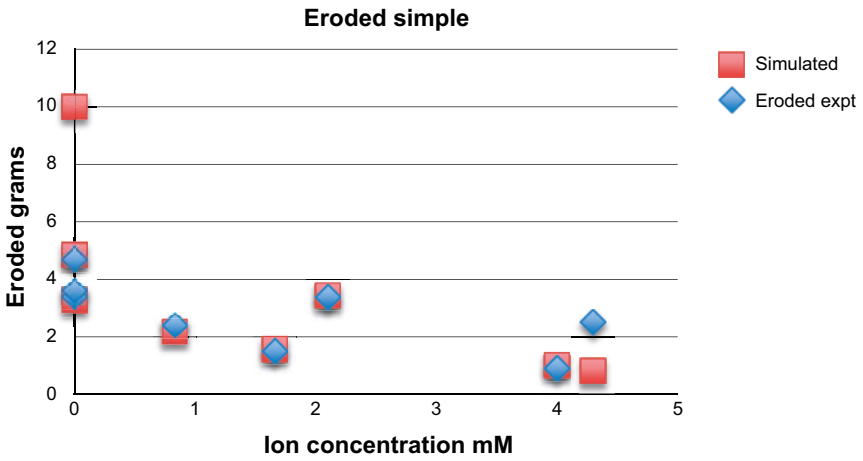

Figure 4-1. *Eroded mass from experiments and simulations as function of ion concentration mM with* $\phi_{R,f} = 0.015$.

When at the end of some of the experiments the fracture was turned from horizontal to vertical, the flocs rapidly sedimented driven by gravity. Simultaneously new small flocs were released from the paste/sol/water interface. Larger flocs catch up with smaller flocs and form larger structures, all visible to the eye, that fill the space between the walls of the fracture and migrate further as irregular coin-like structures. The flocs collect and seemingly form homogeneous sediment at the bottom of the fracture. These experimental observations led to incorporation of floc movement caused by the negative buoyance force acting on the flocs in the erosion model. The model concept is simple. It is based on the observations that at the paste/sol interface the released colloidal particles rapidly agglomerate to form small flocs that sediment. In fractures with apertures larger than the size of the flocs, these sediment as individual agglomerates. In narrow fractures the originally released small flocs join to form a coherent "agglomerate fluid", AF, that is in contact with the fracture walls. The rate of small floc movement is modelled by Stokes law and that of the AF is modelled by the cubic law. This is described in detail in Neretnieks et al. (2016a, Appendix 3). The rate of loss of smectite in a sloping fracture is then modelled by combining the original paste/gel expansion model with the rate of loss by the gravitation driven model (Neretnieks et al. 2016a).

Figure 4-2 illustrates how the clay expands in the fracture and how flocs form, grow and sediment.

Parallel in time with the extension of the model to include flocculation and sedimentation B+Tech made 52 experiments to specifically study erosion under impact of gravity. This was done in fractures at 0, 45 to 90 degree angle from the horizontal. Concentrations covered 0–171 mM NaCl using NaMt as well as NaMt/CaMt in proportion 50/50. Water velocities were 7.1×10^{-6} m/s (230 m/yr) in most experiments with 1 mm aperture fractures. Three experiments were made in a fracture about five times the area of the smaller ones with about the same velocity. Two experiments were made in 0.1 mm aperture fractures, one with 10 times higher velocity and one with stagnant water (Schatz and Akhanoba 2016).

Figure 4-3 shows examples of expanding clay, which releases flocs that sediment in a 45 degree fracture. It is seen that in the narrow fracture the flocs have agglomerated to form a coherent structure that can be broken up in larger sections that move independently. In the larger aperture fracture the small, hardly visible, flocs have not joined into a coherent "agglomerate fluid".

The results support earlier findings qualitatively in several important ways. Erosion is only found at ion concentrations below somewhat less than 10 mM NaCl and for all bentonites with mostly Na as charge balancing ion. Clay expansion into the fractures is observed with all clays up to several cm before again receding when there is erosion and the source is partially depleted. When there is erosion, the rate of erosion seems to be correlated to the area of the clay/water interface i.e. perimeter times aperture irrespective of if the fracture is horizontal or has a slope of 45 or 90 degrees. Sloping fractures practically always give larger erosion rates than horizontal fractures. Similar experiments were made at Ciemat, ClayTechnology and Karlsruhe Institute of Technology, KIT, with similar results.

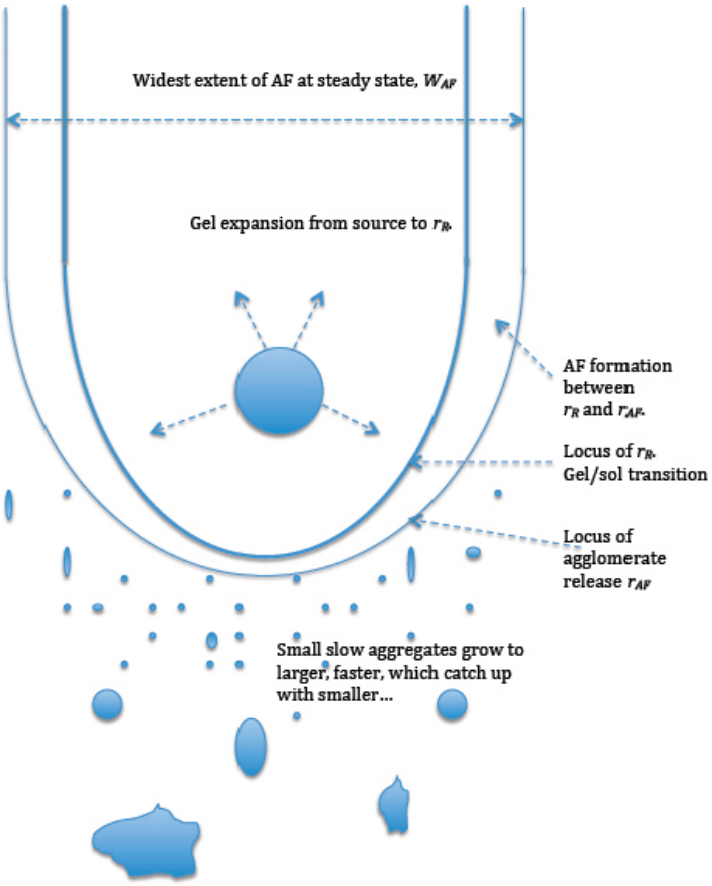

Figure 4-2. *Smectite clay expands in all directions in a vertical fracture and releases agglomerates, which sediment from a boundary at* r_{AF}.

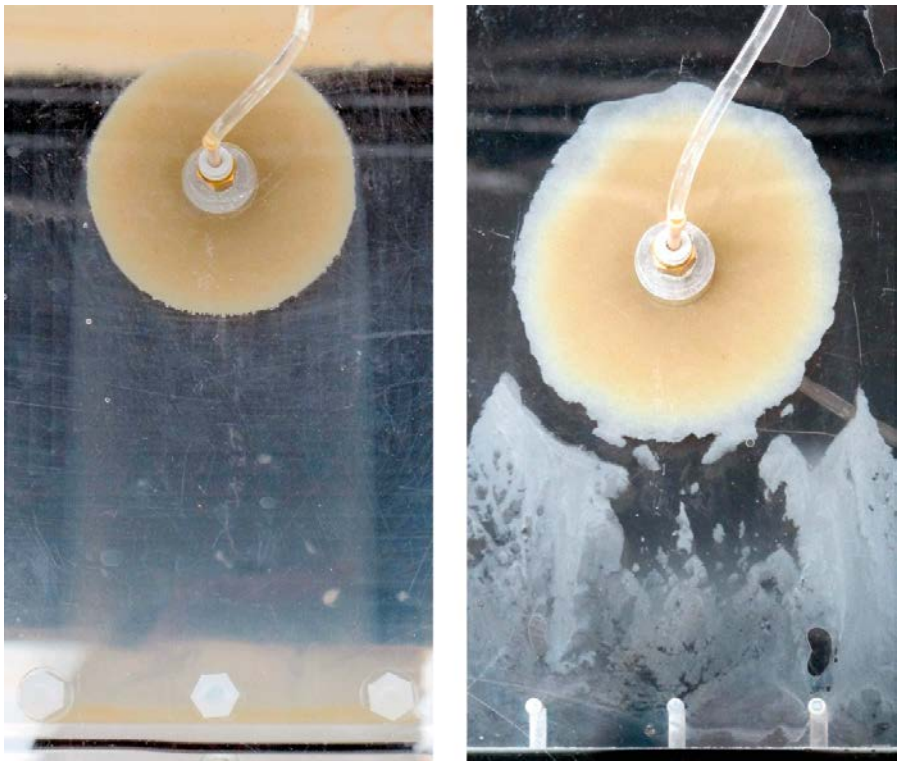

Figure 4-3. *Images of extrusion and mass loss of sodium montmorillonite in 45° sloped fractures with 1 mm apertures, left and 0.1 mm. Simulated Grimsel water, GGWS, with* Na^+ *0.68 and* Ca^{2+} *0.14 mM (Schatz and Akhanoba 2016).*

These experiments have not been modelled quantitatively with the erosion model that accounts for floc formation and erosion caused by sedimentation. However, the overall loss rates expressed as mass per the clay/water interface area ($2\,\pi r_R \times$ aperture) are similar to earlier results.

B+Tech also performed Optical Coherence Tomography (OCT) in which sedimentation of agglomerates in a horizontal 1mm aperture fracture is clearly demonstrated. Figure 4-4 is taken from Figure 14 in D2.11.

4.1.2 ClayTechnology

ClayTechnology made a series of erosion experiments in a narrow plane walled fracture very similar to those made by B+Tech. In these experiments the apertures were 0.12 mm and 0.24 mm respectively. The clays used were purified and mono-ionic MX-80 called WyNa, and WyCa and 50/50 mixtures of them (Hedström et al. 2016). Erosion rates at different flow velocities were reported for deionised water and for NaCl concentrations from 1 to 20 mM. Extrusion distances were typically to a total diameter of 6 cm (3.5 cm pellet expands to 6 cm). In one experiment with 25 mM NaCl in the 0.12 mm aperture fracture no further extrusion was observed after 48 hours beyond 2 mm outside of the original paste in the fracture. This is in contrast to the B+Tech observations in a, much larger, 1 mm, fracture with 171 mM NaCl, also with homo-ionic clay in which expansion reached 27 mm after 700 hours and had not stopped at that time. However, it should be noted that the starting density was lower in the ClayTechnology experiment, 1 260 compared to 1 590 kg/m^3.

Similar observations of erosion in sloped fractures as B+Tech were made. For 5 mM NaCl solutions the results were underestimated by the model that was earlier derived based on B+Tech experiments. This is shown in Figure 4-5. The lines are modelling results. Some details of the experiments were not reported e.g. how long time each erosion rate measurement took and how the paste/sol front evolved during the experiment. In the modelling it was assumed that the front had expanded one radius out from the initial.

Some experimental results, e.g. Figure 21 in D2.11 show that the erosion for 10 mM is as large as for 5 mM for a 0.12 mm fracture. The 0.24 mm fracture has twice the erosion rate as the 0.12 mm fracture for 5 mM. In some tests the same clay pellet was subjected to increasing or decreasing water concentrations in steps of 5 mM spanning ranges from 0 to 20 mM. There were large differences in erosion rates for the same concentrations 5 and 10 mM when they were reached going up or down. This hysteresis effect suggests that the clay has a memory and that there had not been sufficient time to reach steady state conditions.

In contrast, except for the results of Baik et al. (2007) who observed erosion at 100 mM $NaClO_4$, practically all results from the different research groups show negligible erosion for ion concentrations above 5 mM Na^+. Similar to other groups' results erosion increases with water flow velocity and decreases with increasing NaCl concentration but the results are somewhat erratic.

In all test including those with mixed Wy-NaCa and ion concentrations between 1 and 4 mM NaCl, grossly seen, the erosion rates spanned the same order of magnitude as those found by B+Tech under similar conditions in the horizontal fractures.

4.1.3 BELBaR Benchmark tests

Two teams, Ciemat and B+Tech, performed and reported nearly identical experiments in which the same clay, a homo-ionised clay with sodium, Nanocor® expanded into 0.1 mm aperture slots in 1 mM NaCl. During the first 30 days experiments the water was stagnant. The expansion over time is shown in Figure 4-6 together with the simulated results based on the model that was devised inspired by Schatz et al. (2013), series of experiments. The Nanocor clay is not entirely devoid of accessory mineral particles but these are smaller than 0.01 mm according the patent description. The amount of this material is less than 2 %. The B+Tech and Ciemat results are practically indistinguishable. Figure 4-6 shows these results together with the simulated results.

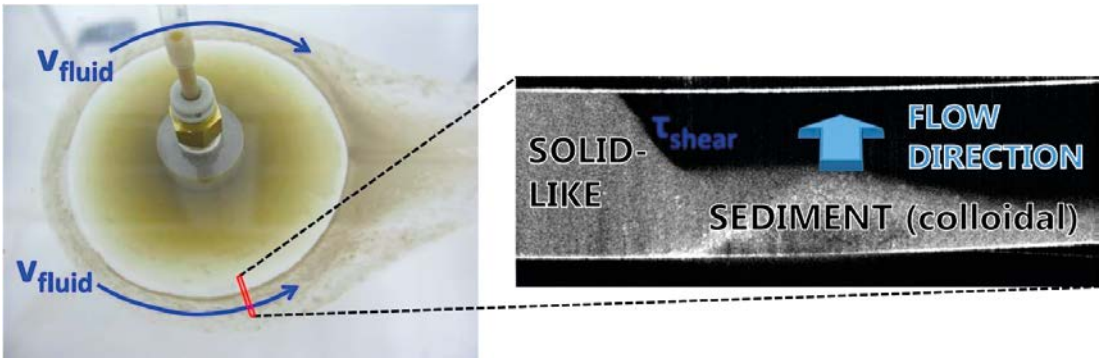

Figure 4-4. *On the left: Overhead photograph of an artificial fracture test. The expanding solid-like phase can be clearly identified as the white-rimmed circular zone slightly to the left of center in the picture. The colloidal (sedimenting) phase is also visible outside of the solid- like phase as a light brown-colored zone that apparently arranges itself along the water flow path. On the right: Optical Coherence Tomography (OCT) image of the region marked with red color in the photograph. The OCT image is a side-view of the interfacial zone from which the sharpness of the solid-liquid interface can be clearly seen.*

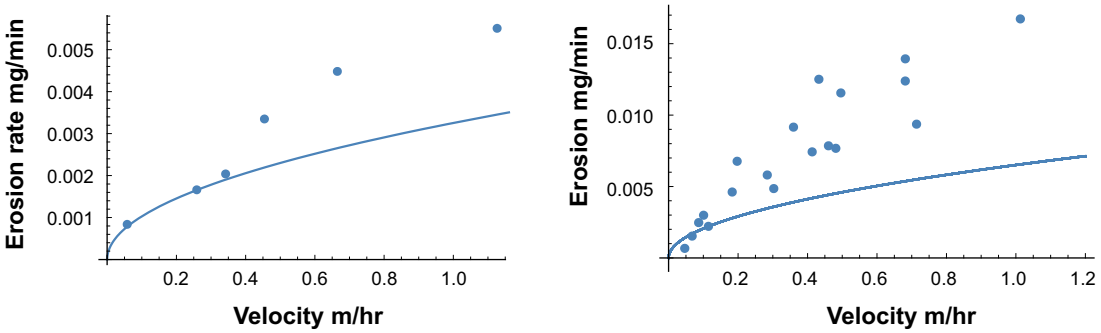

Figure 4-5. *Erosion rate in 0.12 (left) and 0.24 mm aperture slot of Wy-Na with 5 mM NaCl solution. Data from Figures 19 and 20 in D2.11.*

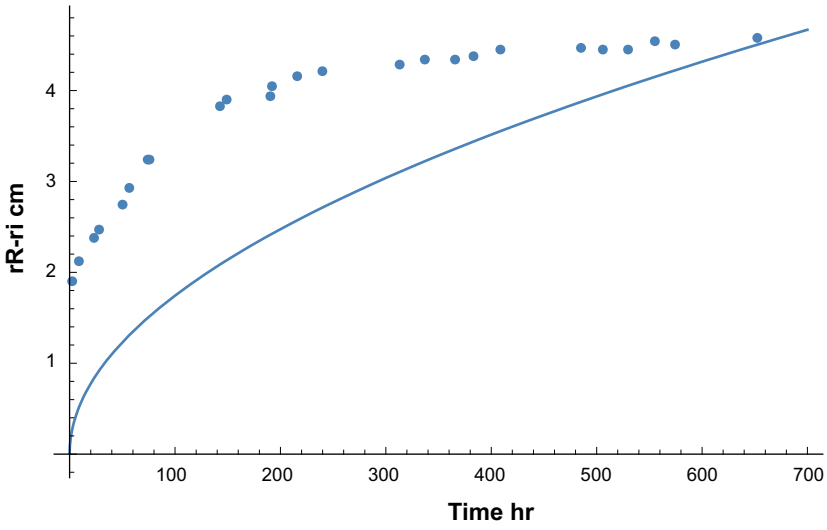

Figure 4-6. *Extrusion of Nanocor® clay into 0.1 mm aperture fracture with stagnant water. Dots are experimental and line is simulated results.*

The experimental results suggest that a steady state extrusion has been attained after about one month. This is in contrast to model predictions, which suggest that the expansion should continue over much longer times, considering that the loss of clay from the source is very slow so far. This is surprising because in the simulations of Schatz et al. (2013) experiments with 1 mm fractures the agreement between model and experiments were much better. However, in those experiments the mass loss was considerable and extrusion slowed down because of the decrease of swelling pressure in the source.

One may speculate that the in a narrow fracture the agglomerates sediment and fill the aperture and this agglomerate fluid, AF, slows down and even hinders further expansion of the swelling clay. See Figure 4-3.

4.1.4 University of Strathclyde.

An experiment with the specific aim to study the clogging of variable aperture fractures by the accessory minerals in the clays was made using a transparent replica of a real granite fracture (Reid et al. 2015). A 26 cm diameter flow cell with a central 2 cm hole hosting a compacted bentonite plug was equipped with a load cell to measure the evolution of the swelling pressure during the experiment. Deionised water passed through the fracture between inlet and outlet on opposite sides of the bentonite plug made of as received MX-80 clay. This contains about 10 % accessory minerals with particles larger than those of the smectite clay. The hydraulic aperture of the fracture was 54 μm The mean mechanical aperture is estimated to be about 250 μm from observed water velocity (5×10^{-4} m/s) by dye injection and fracture size. The water flowrate decreased gradually from about 1.4 to 0.8 ml/min during the 130 days of the experiment. The extrusion increased to 23 mm during this time. The erosion rate varied in cycles of about 40 days with decreasing top erosion rates. After 130 days the erosion rate had decreased about five-fold. The swelling pressure also varied during the cycles. The equipment is shown in Figure 4-7.

The extrusion was followed by a series of photographs. As the rim of the clay expanded and released smectite colloids the accessory minerals were left behind at the rim, forming a barrier the smectite must penetrate to erode. The swelling pressure inside the rim increased as more clay intruded the fracture. The barrier was locally broken allowing an increased penetration rate of smectite particles. Figure 4-8 shows a photograph of the rim with it accessory minerals. The picture is enhanced by an image analysis tool. It is seen that the accessory minerals are left behind at the rim of the expanding clay when smectite colloids outside the rim are carried away by the seeping water.

Figure 4-9 summarises the observations over time of water flowrate, swelling pressure, erosion rate, expansion distance of the mineral rim and the mineral ring area. The erosion rate increases and decreases a few times. This was found to be caused by sudden penetrations of the mineral ring when the increasing swelling pressure inside the ring broke it in weak locations. The picture shows that there exist a few locations where the ring is very narrow and even breached. New accessory minerals are carried by the clay to those locations and repair the breach. The pressure builds up until the ring again is broken. After a few cycles the penetration resistance of the ring had increased sufficiently to build a stable filter everywhere. It is expected that eventually the filter will become as effective as those that build up in the pores of the filters, which have similar pore sizes as the fracture, namely about 0.1 mm (Richards and Neretnieks 2010).

After 130 days the mean width of the ring is 5 mm. One may argue that on the repository scale the mineral ring thickness will be much wider because more clay will have been eroded than the 1.1 g eroded in the experiment. The larger thickness will better withstand the swelling pressure of clay inside it and thus better slow down or stop erosion of smectite particles. There are also observations that addition of kaolinite and quartz sand of different sizes in experiments with clay expanding in fractures show that the mineral particles accumulate at the expanding rim (Neretnieks et al. 2013).

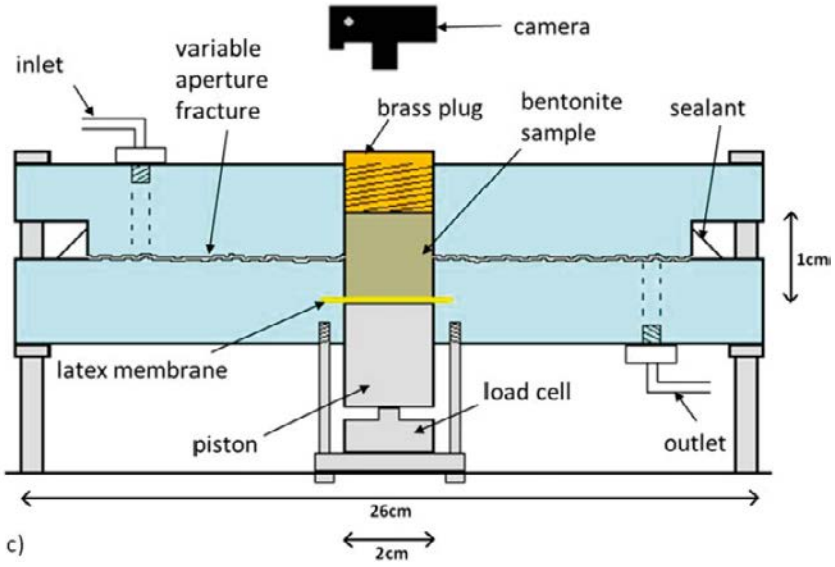

Figure 4-7. *Experimental equipment with artificial fracture (Reid et al. 2015).*

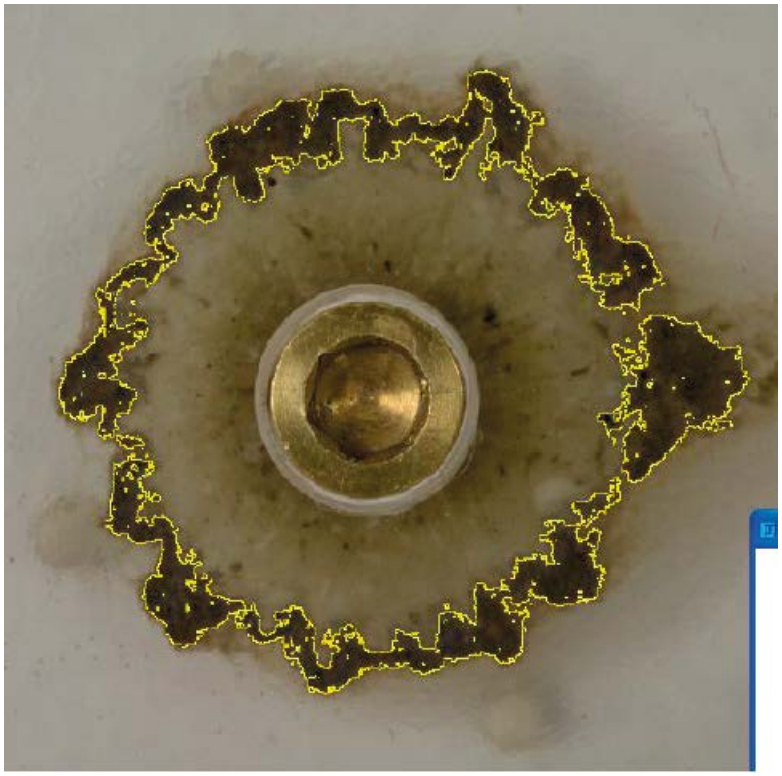

Figure 4-8. *Accessory minerals left behind at the rim of the expanding clay when smectite colloids outside the rim are carried away by the seeping water. The diameter of the source is 20 mm (Reid et al. 2015).*

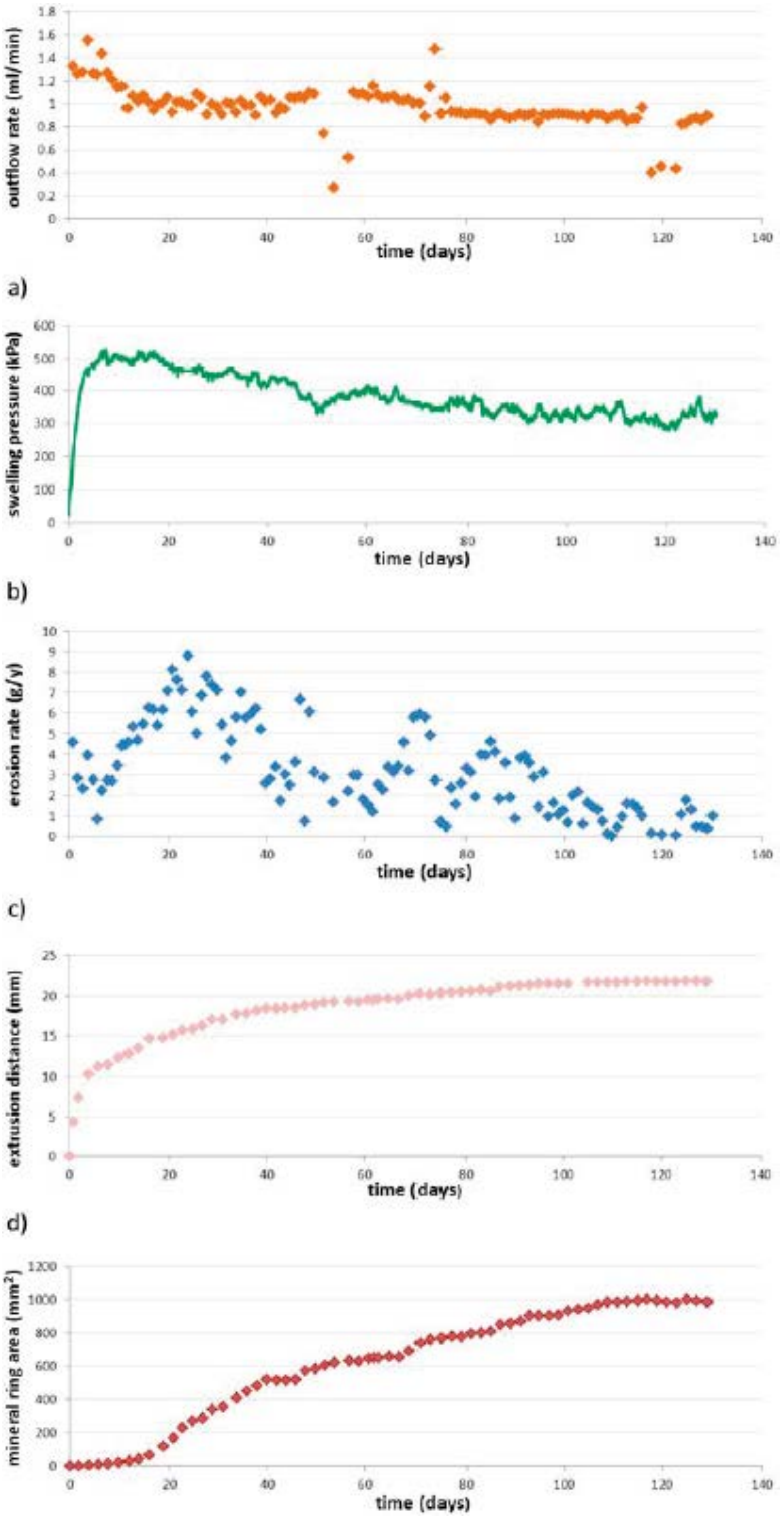

Figure 4-9. *Evolution of water flowrate, swelling pressure, erosion rate, expansion distance of the mineral rim and the mineral rim area over time (Reid et al. 2015).*

Table 4-1 summarizes some of the results of B+Tech , ClayTechnology and Ciemat reported in Missana (2016, Annex). Also Reid et al. (2015) are included. The earlier results of B+Tech (Schatz et al. 2013) essentially are in the same range as those in Table 4-1. These are also shown in Figure 4-1.

Table 4-1. Summary of erosion results in artificial fractures.

Range of experimental times, hrs	Mean erosion flux, kg/m^2/yr	Standard deviation of erosion flux, kg/m^2/yr	Largest erosion flux, kg/m^2/yr	Number of experiments used in this compilation	Clays used	Organisation and comments
641–2 759	257	264	1 288	32 Schatz and Akbanoba (2016)	MX-80 as received, NaMt, CaMt. 50/50, Milos, Kutch	B+Tech Sloping, 45 and 90°, mostly 1 mm aperture, 3 with 0.1 mm, one horizontal fracture. 0 and 1.1–4.3 mM
23.2–168	158	88	240	3 Hedström et al. (2016)	50/50	Clay Technology 2 sloping, one 45°, 0.12 mm aperture. 1.12 mM
360			5.4–208	2 (Missana 2015, Annex)	Febex as received, Nanocor	Ciemat Flow, ionic strength 1 mM,
3 120	190 decreases to 40 over 130 days	–	190	1 Reid et al. 2015)	MX-80	U. Strathclyde Flow, 0.25 mm, DI

It may be noted that all these experiments have been made with a very small diameter source and the radius to the eroding interface has varied from a few cm to less than 7 cm, mostly 3–5 cm. The erosion rate in sloped *smooth-walled, constant aperture slots* (fractures) does not seem to be influenced by the presence of accessory minerals. The sedimentation model predicts approximately these results but only for apertures less than 0.1 mm fracture where it is assumed that a coherent agglomerate fluid has formed. For larger apertures this does not happen according to the experiments and floc *release* and formation rate per area, which is independent of aperture will set the rate of loss. For narrower fractures than 0.1 mm the model predicts the loss to decrease in proportion to the aperture to the third power but there is not sufficient experimental evidence to confirm this. The model is thus essentially based on the empirical data and its validity is not assured for extrapolation.

4.2 Older relevant observations of flow and erosion in fractures

Kanno and Wakamatsu (1991) performed expansion extrusion and erosion experiments in transparent fractures between 0.3 and 1.5 mm aperture with as received Kunnigel V1 bentonite and 70/30 mixture of bentonite and sand using distilled water. They found extrusion distances of the swelling bentonite between 15 and 50 mm after a few thousand hours and that the expansion was proportional to the square root of time. The expansion was larger for the larger aperture fractures. Their model is based on the balance between swelling pressure and friction of the water intruding the clay and is formulated as a diffusion process. They also invoke friction of the expanding clay against the fracture walls, which suggests that the expansion rate should be proportional to the aperture squared. This would imply that their expansion should be 25 times larger for the larger fracture. This is not found in their experiments although they do find a difference somewhat larger than 3.

Baik et al. (2007) used a granite cylinder 0.285 m long with 0.1 m diameter intersected axially by a fracture in which water can flow. At the inlet end a cylindrical cavity 100 mm long with a diameter of 54 mm is filled with a bentonite block. The bentonite has 70 % montmorillonite, 29 % feldspar and 1 % quartz. The bentonite block is in contact with the 0.51–0.59 mm aperture with flowing water. The swollen bentonite was found to have intruded 3 mm into the fracture after the experiment. Three flowrates were used 0.001, 0.01 and 0.1 ml/min. In all experiments the effluent particle concentration dropped rapidly over time. Surprisingly the 0.1 M NaClO4 gave the highest concentrations around 20 mg/l. With the 0.001 and 0.01 M the concentration stabilised at around 5 mg/l. Considering that the loss of montmorillonite during an experiment was very small compared to the inserted mass it cannot be a loss of swelling pressure that caused the decease in loss with time.

The duration of the experiments was 100 000 minutes (1 700 hours) for the 0.001 ml/min flowrate, 1 000 hours for the 0.01 ml/min and 83 hours for the 0.1 ml/hr case. Considering that extrusion distances in other experiment are on the order 10–40 mm under especially the low ionic strength case, 1 mM, it seems reasonable to assume that the 30 % accessory minerals left behind or intruding the fracture formed a filter near the fracture inlet. This supports the findings presented later in the present report, that accessory minerals can seriously reduce bentonite loss for a deposition hole.

Vilks and Miller (2010) performed erosion experiments in transparent fractures, 1 and 5 mm aperture, as well as in a Quarried Block tests. Some specific aims were to explore if fractures could be clogged with erosion resistant mineral deposits from the expanding bentonite and if gravity could induce loss of clay in sloping fractures. They used as-received Wyoming bentonite WyBt, as well as Na-exchanged, NaMt, and Ca-exchanged CaMt bentonites. Deionised, and synthetic so-called Grimsel water with Na 1 mM and Ca 0.2 mM mM were used. In the erosion experiments with the as-received WyBt with DI as well as Grimsel water in 1 and 5 mm fractures the expanding clay left the accessory minerals behind as a ring as the Mt was carried away be the seeping water. In the 15° dipping, 1 mm aperture sloping fracture with WyBt as well as with NaMt, sedimenting flocs of Mt were at first moving downslope but stopped as bentonite deposits became fixed to the fracture. The flow direction of the flocs was somewhat influenced by the cross-flowing water. In the sloping fracture the down-slope movement of bentonite stopped as bentonite deposits became fixed to the fracture surfaces.

In the test with CaMt and Grimsel water the expansion distance was similar to that in the other tests but the downstream water was essentially free of particles.

In the test with 5 mm aperture fracture, with WyBt and Grimsel water the clay expanded about 25 mm in 267 hours. The same distance was reached with NaMt in 1 mm aperture fracture after 432 hours. These distances are comparable to the distances found in Schatz et al. (2013) for comparable situations. It may be noted that there are no noticeable difference between 1 and 5 mm fractures.

The Quarried Block is a 1 m × 1 m × 0.7 m block of granite containing a single, well-characterized, through-going variable aperture fracture. Two WyBt plugs intersecting the fracture in different locations were exposed to Grimsel water flow. The migration of colloids from the sources could be followed by the added synthetic fluorescent colloids. 18 boreholes that intersected the fracture were used for monitoring. The fracture aperture varied mostly between 0 and a few mm but there were pockets with up to 10 mm aperture in several places. Tracers were used before and after bentonite erosion tests. They revealed significant changes in transport properties after the bentonite erosion tests. The changes in fracture transport properties suggest that bentonite deposition in the fracture had taken place. Post-mortem analysis showed that small amounts of smectite could be found deposited on the fracture surfaces, mostly in the vicinity of where the bentonite plugs were located.

4.3 Rheology of montmorillonite suspensions

The expanding clay in the fractures forms an inner region with a volume fraction larger than about 2–3 %. This paste has so large shear strength and/or viscosity that it is not deformed and does not flow by the hydraulic gradient or gravity (Eriksson and Schatz 2015). At the rim of this region individual montmorillonite particles are released when the ionic strength is below about 4–10 mM. Partly these agglomerate, given time, and settle by gravity to the lower side of the fracture. In more sloping fractures the agglomerates can sediment along the fracture. The newly settled agglomerates seem to be carried by the water without much influence on the water flow as was found by adding dye to the seeping water (Eriksson and Schatz 2015, Supplement, Figure 1). However, it is likely that the agglomerates develop stronger space filling structures over time and gain a shear strength that potentially could slow down or even stop the agglomerate fluid, AF, movement as shown in Figure 4-3. Very few measurements of AF viscosity or shear strength with around 1–4 volume % Mt have been reported for slurries that have been left standing for many days or months. On the contrary, to ensure that the slurry is homogenised before the measurement it is vigorously shaken. This destroys any built up 3-dimensional structures. For 1 volume % NaMt in 1 mM NaCl the slurry viscosities for NaMt as well as for 50/50 Na/CaMt were around 0.01 Pas. This is fully in line with

what sol has under these conditions (Liu 2011) and suggests that the montmorillonite particles are essentially delaminated. The yield stress of 0.5 and 1 % montmorillonite measured under shear rates from 1–1 000 s^{-1} were between 0.01–0.1 Pa for 1 mM NaCl for NaMt as well as for 50/50 Na/CaMt. Hedström et al. (2016) using purified montmorillonite from Asha bentonite that had rested 24 hours found yield stress of 0.4 Pa for a suspension of 0.37 volume %. It increased to 1.1 Pa after 1 weeks aging. The ionic strength was above CCC. For 0.75 volume % the yield stress was 4.4 and 7.7 Pa. Clearly there is an effect of aging.

Vigorous shaking before measurements destroys any built up 3-dimensional structures. To obtain the desired information measurements must be made at extremely low shear rates and reasonably low strain. Such measurements were made by Eriksson and Schatz (2015). The viscosity of a few samples with 1 volume % montmorillonite was measured at low constant shear rate (0.003 s^{-1}) over a 12 h period. Strain amplitude sweeps were performed at strains ranging between 3×10^{-6} and 0.03 radians at a constant frequency of 0.1 Hz. For NaMt the viscosity gradually dropped from nearly 100 Pas to just above 1 for a cumulative shear from 0 to 139. For 50/50 Na/CaMt it was practically constant just below 1 Pas (Eriksson and Schatz 2015, Supplement). Considering that the viscosity of water is 0.001 Pas it can be expected that an AF filling a fracture has a potential to considerably slow down the migration of the AF in narrow fractures. Aging during 12 hours may be a short time for stronger space filling structures to develop, considering that in the experiments in fractures with flow, it took much longer time to see any developed flocs (Schatz et al. 2013). A short overview of earlier work on rheology of clay suspensions is presented in Section 6-3 in the context of the subsequent fate of the eroded material and the impact for performance assessment

4.4 Tentative conclusions from the erosion experiments in fractures and filters with homo-ionic clay devoid of accessory minerals

The colloidal particles readily penetrate narrow pores in filters irrespective of pore size above 2 μm with the same rate, which is in agreement with theory and earlier experiments (Neretnieks et al. 2009).

The experiments confirm that at ion concentrations above 5–10 mM sol formation does not occur. At higher concentrations erosion does not take place in horizontal or sloping fractures with or without flow. This is in good agreement with theory.

At ionic strengths below 5–10 mM homo-ionic clay with at least 20 % Na compensating the structural charge of the smectite, sol forms at the paste/sol interface and can be carried away by seeping water as sol or as loose flocs formed by agglomeration of the smectite particles. In inclined fractures flocs, which are slightly denser than water sediment rapidly. Floc formation considerably increases erosion in flowing horizontal fractures. In sloping fractures considerable erosion is induced by sedimentation of flocs also in stagnant water.

The model that accounts for flocculation and sedimentation was developed largely using the experimental findings by Schatz et al. (2013). The new data obtained by Schatz and Akhanoba (2016) in 1 and 0.1 mm fractures and ClayTechnology in 0.12 and 0.24 mm horizontal fractures, gives similar results and supplement the earlier results and support the idea that the erosion loss increases linearly with the aperture. It is acknowledged that there are considerable variations in the experimental results but the uncertainties are mostly within an order of magnitude in the concentration span 1–200 mM and 0.1–1 mm aperture for the homo-ionic purified MX-80 clays studied.

We re-emphasize that the all but one experiment were made in smooth walled slots in which the accessory minerals do not get trapped as they would in narrow or even closed locations in real fractures with varying apertures. The experimental results with homo-ionic clays have their great value in that they show that the underlying theories, mechanisms and processes in the models for smectite paste/gel/sol behaviour are not contradicted and in many cases they support them well.

5 Erosion experiments with filters

5.1 Clays devoid of accessory minerals

ClayTechnology (Birgersson et al. 2009) report a series of experiments in which compacted, as received, MX-80 as well as Na-homo-ionic accessory mineral free smectite, called WyNa is sandwiched between two filters flushed by water. Smectite that migrates through the pores of the filters are carried away by water circulating on the outside of the filters. Figure 5-1 shows the experimental setup. Deionised water was used in the circulation circuit.

The filters were 2mm thick and had pore sizes ranging from 0.2 μm to 100 μm Porosities ranged from 12–55 %. The change in swelling pressure was monitored over time as well as the turbidity caused by smectite in the circulating water.

Typically no loss of swelling pressure was seen with 0.2 μm filters, which is not surprising because the smectite particles are around 0.2 μm. The 2 μm filters allowed smectite colloids to pass and swelling pressure to decrease from 6.5 to 1 MPa in 20 days with WyNa but with MX-80 the pressure dropped from 5 to 3.7 MPa during the same time. A 10 μm filter exhibited essentially the same pressure loss over time as the 2 μm filter for WyNa. Turbidity measurements of the circulating water showed that MX-80 releases orders of magnitude less smectite than WyNa. This suggests that the accessory minerals clog the filters. See Section 5-2 on experiments specifically dedicated to clays with accessory minerals.

The swelling pressure decline due to loss of smectite from the source could be well predicted for the WyNa tests by the dynamic smectite-swelling model. This is based on force balance of DDL, VdW and friction forces between smectite particles and water. The predictions were made without using any adjustment of parameters (Neretnieks et al. 2009). No friction between the smectite sol and the pore walls in the filters was invoked as the dynamic model predicts that this should be negligible. This is also proven by the fact that 2, 10 μm and 100 μm pore sizes have negligible impact on the rate smectite loss through the filters.

The mean flux during the experiments was estimated to be on the order of 20 kg/m^2/yr, based on the decrease in clay density with swelling pressure,

The findings that MX-80 exhibited much smaller pressure decrease and clay loss was attributed to be caused by the presence of accessory minerals causing pore clogging (Neretnieks et al. 2009).

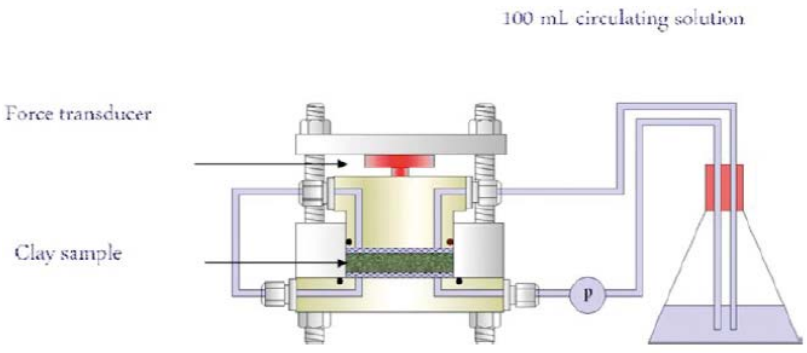

Figure 5-1. *Experimental setup with compact clay sandwiched between filters flushed by circulating water.*

5.2 Erosion experiments with clays that contain accessory minerals

The clays to be used as buffer and backfill materials in the nuclear waste repositories contain 10 % by weight or more of other mineral particles, which have particle sizes between 1 and 100 μm (Richards 2010, Neretnieks et al. 2013). These are called accessory minerals or detritus. It was shown that minerals with such size distribution when forming filters a few mm thick effectively hinder smectite particles, which have the form of thin sheets with a few hundred nm size and 1 nm thickness to pass. It was suggested in Neretnieks et al. (2009) that these minerals would be carried along by the expanding smectite in the clay until the smectite formed a dilute sol and could no longer push them further. In variable aperture fractures the minerals would soon collect, form filters and slow down and eventually stop further erosion. However, there was not sufficient experimental evidence to ascertain that this would occur as pointed out by Apted and Arthur (2012) and the mechanism was not invoked in the safety analyses of SKB and Posiva (SKB 2011, Posiva 2012).

In the BELBaR project several groups systematically addressed this possibility. Ciemat used as received clays and homo-ionic clays retaining the accessory minerals in a series of tests in which compacted clay tablets between porous metal filters allowed water to wet the clay and smectite particles to escape through the pores of the filters. Experiments with no flow as well as flow through the filter in the direction perpendicular to the swelling direction were made (Neretnieks et al. 2013). Rapid clogging of filters was observed with filter pore sizes between 2 and 100 μm for both flow and stagnant filter experiments decreasing erosion by several orders of magnitude compared to the former ClayTechnology experiments with no accessory minerals described in Section 5-1. Details of these experiments are discussed later in this section.

Clogging effects are clearly seen in the experiments at Ciemat (Missana et al. 2011). In these experiments the accessory minerals were always present in the compacted clays, the as received as well as the homo-ionic clays.

A series of experiments were made with water-saturated bentonite under stagnant water as well as flowing water conditions in which as received compacted FEBEX bentonite was confined by porous filters. The same experiments were also made with homo-ionic Na- and Ca-clays and mixtures thereof. The latter clays although fully ion exchanged retained the accessory minerals originally present in the clay. Probably some of the more soluble minerals salts had been dissolved in the homo-ionisation process.

In the first type of experiments a compacted clay sample is sandwiched between two porous stainless steel filters. This package is immersed in a stagnant water volume. See Figure 5-2.

5.2.1 Static experiments (no-flow)

Different waters were used but they all had ionic strength and compositions such that the colloids formed and were stable. In static experiments with as-received clay, during 500 hours, periodic sampling of tiny water volumes was made. This showed that smectite concentration increased and reached a constant concentration after about 50 to 200 days. The clay mass confined between two filters was 4 g and water volume 200 ml outside the filters confining the clay. For initial compactions of 1.6, 1.4 and 1.2 g/cm^3 the concentrations became constant reaching 100, 40 and slightly more than 10 ppm smectite. The two filters, one on each side of the clay tablet were 3.1 mm thick and had a porosity of 40 % and a pore size of 100 μm. More than 30 experiments gave similar results. Filters with 100, 10 and 2 μm pore size gave similar results provided the porosity was the same (Missana et al. 2011).

Figure 5-3 shows how the smectite concentration in the surrounding water increased and reached a constant value after 50 to 200 days for 6 different as-received clays in deionised water, DI. Waters with 10 mM NaCl gave about 10 times lower release and the simulated Grimsel groundwater with NaCl and a small fraction $CaCl_2$ with together less than 1 mM gave about 3 times lower release than DI. It may be noted that one of the clays, Nanocor, contain very small amounts of accessory minerals but still clogs the pores.

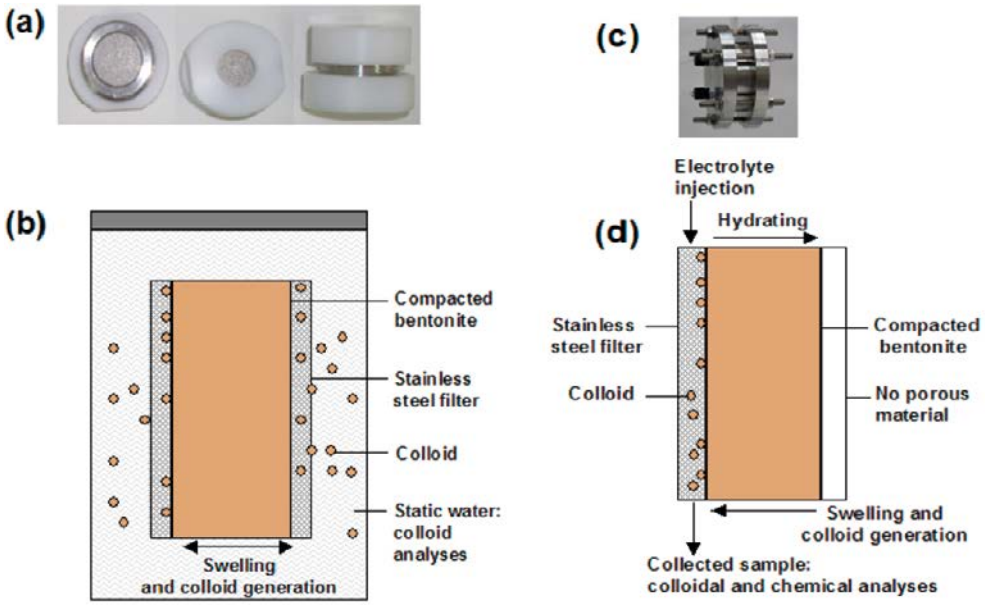

Figure 5-2. *Schematic representation of erosion tests with confined clay, a and b) static (no-flow); c and d), dynamic tests (flow through filter) (Missana 2016).*

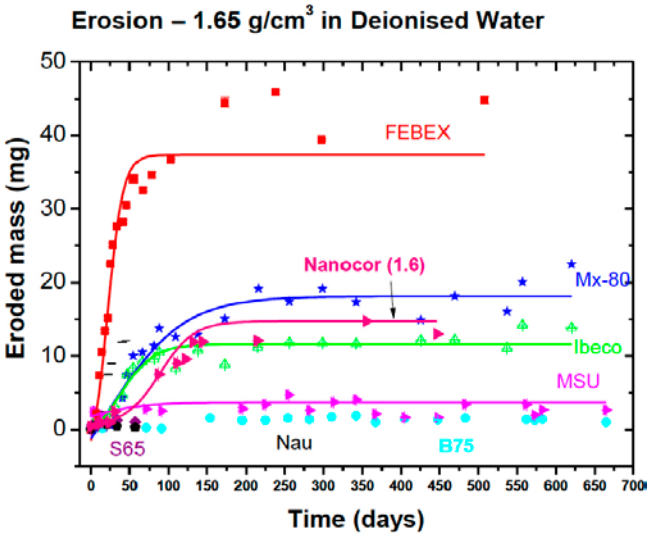

Figure 5-3. *Eroded mass measured as function of time in deionised water from different raw bentonites compacted to 1.65 g/cm^3 in non-flow tests (Missana 2016).*

The final concentrations (20–100 ppm) Missana et al. (2011) were interpreted by the authors to be *equilibrium* concentrations and it was suggested that this could be used to estimate the maximum rate of smectite loss to flowing water. This interpretation contradicts observations that swelling clay under solubilising condition can reach much higher concentrations. Unless impeded by gravity in e.g. upward swelling clay in a test tube, clay should fully disperse in available water. We interpret these results to show that after an initial loss of smectite through the filter the pores at the inlet have been clogged and essentially do not allow more that extremely small amounts of smectite particles to pass.

A number of the Ciemat and KIT filter static (no-flow) experiments with as received as well as homo-ionic Na-clays are reported in BELBaR Deliverable D2:11 (Missana 2016). The mean erosion flux data are summarised in Table 5-1.

Table 5-1. Summary of erosion results through filters.

Range of experimental times, hours	Erosion flux, kg/m²/yr*	Standard deviation of erosion flux, kg/m²/yr	Largest erosion flux, kg/m²/yr	Number of experiments used in this compilation	Clays used	Organisation and comments
1 080–14 880	0.11	0.16	0.56	12 Missana (2016)	Febex as received, Na and Ca homo- ionic, MX-80, Mylos, B/5-CzR, MSU-Russia, all with accessory minerals except Nanocor	Ciemat, No Flow, 100 *μm* filter, 40 % porosity, ionic strength 0.01–20 mM, stagnant
7 800	0.14	0.17	0.37	4	Febex as received, Na and Ca homo- ionic, with accessory minerals	KIT, 10 *μm* filter, 29.4 % porosity Ionic strength 1.6 mM. Flow conditions
480	1.1		1.1		MX-80 with accessory minerals	ClayTechnology, DI and Na/Ca < 1 mM alternating
480	~ 20	–	–	2	WyNa, Note that this experiment had no accessory minerals	ClayTechnology, 2 and 10 *μm*, 30–40 % porosity, deionised water,

* This is based on the area of the filter times its porosity. In the static experiments the erosion rate is derived from the initial slope of loss over time from experiments such as shown in Figure 5-3. As the rate decreases to zero in less than a year and erosion stops the former rate cannot be used to extrapolate to longer times than a year.

5.2.2 Dynamic experiments with flow in filters

In this type of experiment a filter is in direct contact with the compacted clay and water flows *through* the filter parallel to the filter/clay interface and brings with it colloids that have penetrated into the pores.

The effluent concentration of colloidal particles shown in Figure 5-4 is very low and erratic even for the 0.1 mM sodium chloride water (Missana et al. 2011). It can be speculated that floc formation builds up but is occasionally broken up by the flowing water and restarts in the same cyclical was as observed by Reid et al. (2015), described earlier. The flow in the filter experiment is generated by a peristaltic pump and probably has quite constant flowrate. The colloid concentration is much below that observed in experiments in which the flowing water is in direct contact with the clay (Schatz et al. 2013). Clearly, filters can have a strong impact on the rate of release of smectite colloids from compacted clays. This was also demonstrated by Richards (2010) and Richards and Neretnieks (2010) in which one or a few mm thick filter of accessory minerals practically stopped the penetration of smectite colloid particles.

Figure 5-5 shows the results of the experiments performed under dynamic conditions with FEBEX bentonite compacted to 1.65 g/cm^3. Three different electrolytes were used (NaCl, $CaCl_2$ and mixed Na/Ca, all with I = 1 mM). The water flow rate was 20 cm^3/day except for the last few points when the flowrate was raised by a factor of thirty. The flux is essentially constant and is largest for NaCl water. For NaCl it is 0.02 kg/m^2/yr.

These experiments were made with as-received bentonite. Similar experiments with Na-exchanged and purified bentonite with no accessory minerals resulted in a many orders of magnitude larger erosive loss as described in an earlier section (Birgersson et al. 2009). This again suggests that these minerals form filters that let colloid particles pass with great difficulty.

Results of another experiment over 450 days are shown in Figure 5-6 in which the water velocity was changed from 2.4×10^{-8} m/s to 1.2×10^{-7} m/s after 230 days. It is not obvious why the erosion rate dropped considerably when water velocity was increased. Averaging these data over the entire period and for both velocities the flux is 0.01 kg/m^2/yr.

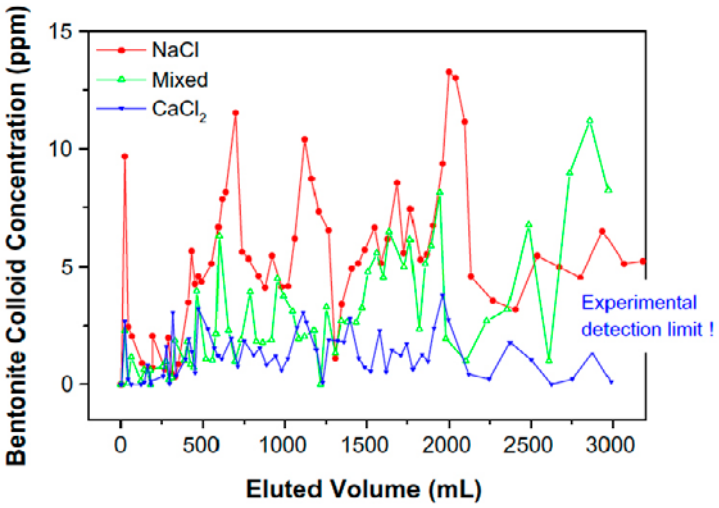

Figure 5-4. *Bentonite concentration in the effluent vs. eluted volume in the experiment with flow through the filter (Missana et al. 2011).*

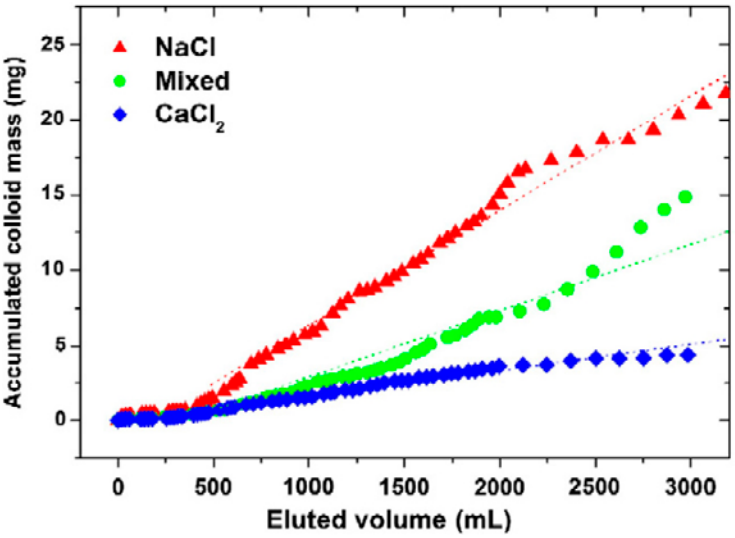

Figure 5-5. *Cumulative colloid mass that has penetrated the filter in different waters (Albarran et al. 2014).*

Experiments in which several successive changes of water composition and flow rates were made were also performed. Figure 5-7 shows the accumulated masses eroded from FEBEX bentonite subjected to flow changes with mixed Ca and Na electrolyte at 1 mM in two different cells, C3 and C4. Water velocities varied from 1.5×10^{-8} m/s to 3.5×10^{-6} m/s. In both cells the erosion rate decreased over the more than 3 years of the experiments. The rates seem not to be influenced much by the changes in flowrates. It was observed that the continuous calcium supply inhibited colloid erosion, possibly caused by ion exchange. For the period from 200 to 1 000 days and for both experiments the flux is 0.0008 kg/m^2/yr.

The maximum erosion flux measured under different experimental conditions is summarized in Table 5-2.

Table 5-2. Maximum eroded flux (kg/m2/yr) measured under different experimental conditions (Neretnieks et al. 2013).

	Initial	Consecutive	flows –>	–>	–>
Velocity m/s	1.1×10^{-7}	1.8×10^{-7}	5.3×10^{-7}	1.1×10^{-7}	1.8×10^{-8}
NaCl, 1 mM	3.94×10^{-2}				
NaCl + $CaCl_2$, 1 mM	1.22×10^{-2}	7.70×10^{-3}	5.20×10^{-3}	1×10^{-3}	1×10^{-3}
$CaCl_2$, 1 mM	6×10^{-3}				

The experiments with flow show that penetration of colloids into pores of the filter, from which they are flushed by flowing water, occurs. Although the loss is small, it does not stop in contrast to what the static experiments suggest. One can speculate that this can be due to the shear forces generated by the pressure drop in the narrow (0.1 mm) pores in the filter.

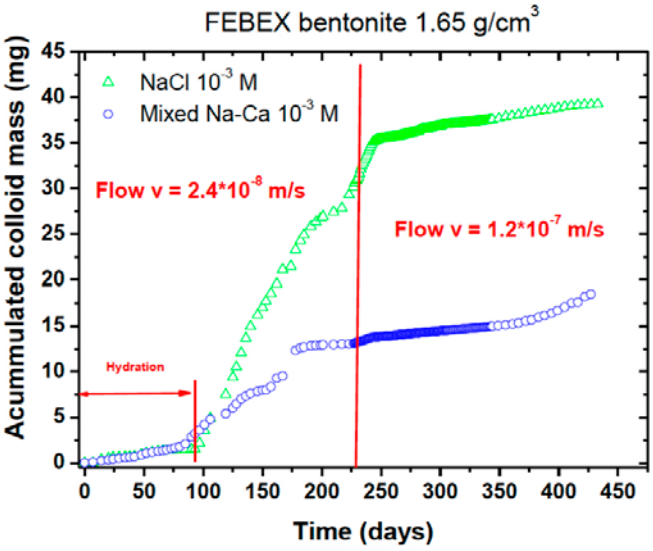

Figure 5-6. Cumulative smectite mass vs. time for two different water compositions (Neretnieks et al. 2013).

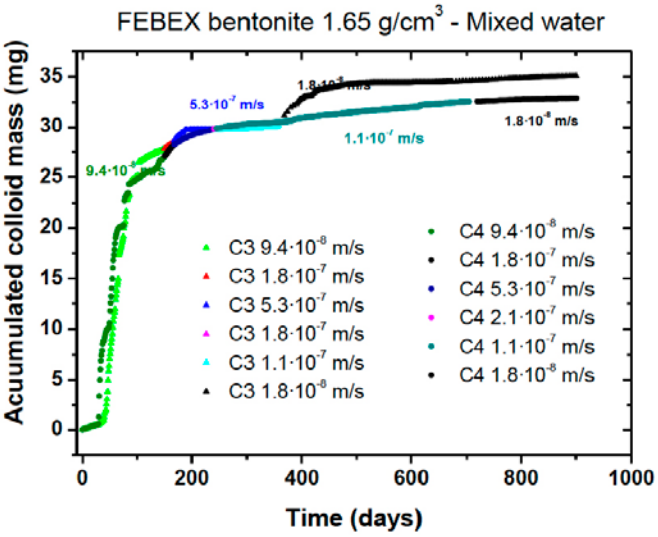

Figure 5-7. Cumulative smectite mass vs. time influenced by flow velocity (Neretnieks et al. 2013).

5.3 Some comments on clogging of filters

5.3.1 Other observations of impact of extraneous minerals

Experiments with addition of extraneous minerals in the form of fine particles, kaolinite clay, $CaSiO_2$, TiO_2, Al_2O_3 and SiO_2 have shown that already a few mm thick layers can effective stop smectite penetration (Richards and Neretnieks 2010).

Filtration is common process to separate liquid or solid particles from gases and liquids and is used in many different contexts. Invariably the problem of clogging is encountered as more and more particles collect and in or on the filter medium. Clogging by colloid deposits is important in water treatment filters, groundwater aquifers, cleaning of air and fuels, medical applications etc. Sodium as well calcium montmorillonites are known to clog sand filters, the former much more rapidly (Mays and Hunt 2007). Clogging of soils preventing sufficient drainage has been recognised to be a major problem in subsurface constructions (Reddi et al. 2000). The literature abounds with papers on clogging of filters but it seems to be difficult to prognosticate the process. Empirical approaches are used to monitor and prognosticate, see e.g. Eker et al. (2016), Petitjean et al. (2016) and Mays and Hunt (2007). There have been attempts to predict clogging using pore network models, e.g. Redner and Datta (2000) that give some insights in the processes involved. It seems that clogging is difficult to avoid in natural soils where there is seepage of water. Recent developments in extended discrete element modelling methods, XDEM, by which the movement of individual particles among a multitude of particles can be modelled driven by flow, gravity and other forces e.g. vdW and coulombic forces have good prospects of modelling filter clogging. Such modelling could give further insights and support to the experimental findings.

6 Implications for repository conditions

In this chapter we first illustrate how the observations described earlier could be used to assess how fast the clay could be lost from deposition hole by direct extrapolation of the rates found in experiments. In the first section the presence of accessory minerals is assumed not to have any impact, In the following section the potential impact of the accessory minerals forming filters at the entrance of and in the fractures is discussed. The section thereafter addresses the fate of the erode material and how this could influence the rate of loss by filling up the fractures. If the lost material cannot be transported away as rapidly as it is released from the tunnels and deposition holes the loss rate will be limited by the far field transport rate.

6.1 Clays without accessory minerals

Refer to Table 4-1. The erosion flux found experimentally by three different groups covering a wide interval of water velocities and water compositions below 10 mM Na^+ are on the order of several hundred kg/m^2/yr in fractures with apertures from 0.1 to 1 mm. Thirty-five experiments were made in simulated fractures with smooth walls. The clays used were cleaned of accessory minerals. Similar rates we found in earlier experiments. The experiments include horizontal as well as sloping fractures.

6.1.1 Loss-limitation by gravity induced erosion

The release rates in the Schatz and Akhanoba experiments range from a few hundred to above 1 000 kg/m^2/yr, (Table 4-1). For so high rates the expansion of the clay into the fracture is only a few tens of cm according to the model described in Neretnieks et al. (2016a). The area for the loss is the aperture times the circumference of the expanded clay, which is just slightly larger than the circumference of the deposition with radius about 1 m. A=$2\pi \times 1 \times$ aperture m^2. The loss then is on the order of 1 000 kg/m^2/yr $\times 2\pi \times$ aperture/1 000 with aperture in mm. This is 6.3 $\times$ aperture kg/yr. For an aperture of 0.1 mm the loss is 0.6 kg/yr for a vertical fracture. However, this mass must be able to flow away in the fracture. As mentioned in Section 4-3 the agglomerate fluid is expected to be more viscous than water and my flow less rapidly than water. This is treated in the following section.

6.1.2 Loss-limitation by viscous aggregates sedimenting in fracture

In the erosion model described in Neretnieks et al. (2016a) it is assumed that the agglomerate fluid has the same viscosity as water and that it readily can flow way. This is based on the interpretation of the experiments described in Schatz et al. (2013) where this was observed. However, in the later experiments by Schatz and Akhanoba (2016) with the 45 degree dipping fractures and the vertical fractures it was found that in narrow fractures (0.1 mm) the sediment agglomerated and formed large sheet-like structures that sedimented slowly. See Figure 4-3. In the sedimentation model of Neretnieks et al. (2016a) it was shown that a high viscosity of the agglomerate fluid, AF, could limit the erosion when it cannot sediment away as rapidly as new smectite could erode at the clay/water interface. Figure 6-1 shows the erosion if it is NOT limited by the loss-rate 1 000 kg/m^2/yr, the full line. The dashed lines show how much AF can be transported away by sedimentation if the viscosity of the AF is 100, 1 000, and 10 000 larger than that of water. For the largest aperture 0.1 mm this could limit the loss rate driven by gravity by several orders of magnitude for the higher viscosities. Highly non-Newtonian suspensions that have a yield strength may even entirely clog the fractures and stop flow altogether.

A short overview of rheology of smectite suspensions is given in Chapter 7.

In larger fractures and fracture zones that intersect a horizontal drift the clay loss could be expected to be orders of magnitude larger.

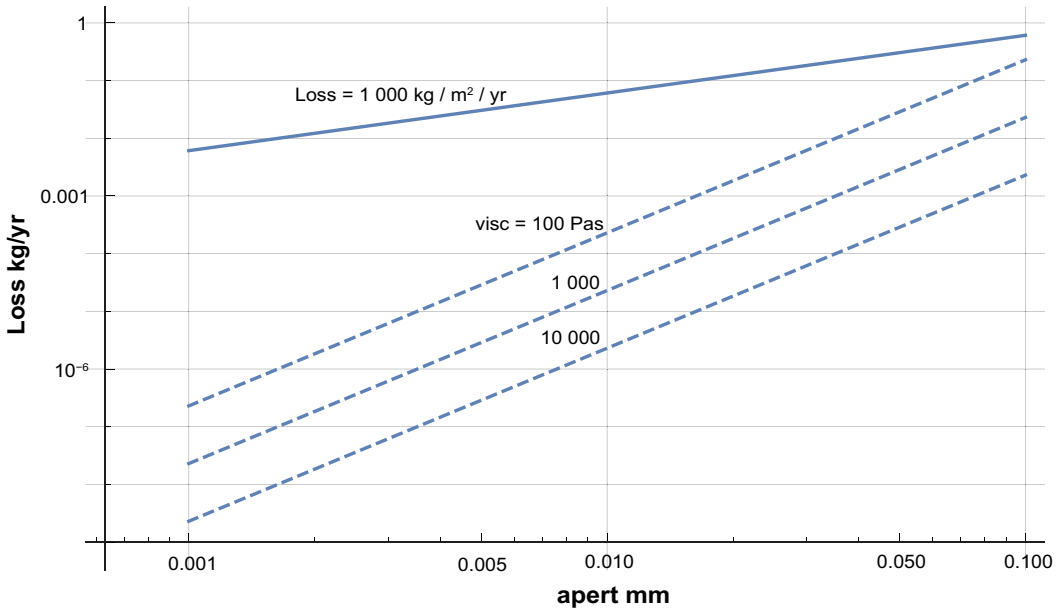

Figure 6-1. *Smectite loss as function of aperture when release rate determines and when sedimentation rate of viscous AF limits loss.*

6.2 Clays with accessory minerals

6.2.1 Experiments with flowing fractures

Refer to Table 4-1. (BELBaR D2.11 Annex) in two experiments found erosion flux of 5.4 and 208 kg/m^2/yr. in experiments in which the water velocity had been increased by a factor of 5 the last 15 days of experiments, which had the first 30 days had stagnant water, and 15 days the lower velocity. In the first 15 days with flow, erosion flux had been 0.31 and 0.35 kg/m^2/yr. There is no additional detailed information documented on these experiments. The results are deemed not to be representative of long-term erosion because the initial erosion flux is quite low, <0.4 kg/m^2/yr, and then when flowrate is increased from 1.4×10^{-6} to 9.34×10^{-5} m/s the fluxes increase by a factor 17 and 590 respectively in the two experiments.

In the U. Strathclyde experiment with an artificial fracture with variable aperture the erosion flux decreased from 190 to 40 kg/m^2/yr and was expected to decrease further as additional accessory minerals build up over time in the ring.

6.2.2 Experiments with filters

Referring to Table 5-1. Note that the filters used mostly had pore size 100 μm. This is within the range of aperture sizes expected in fractured granite at repository depth.

The results presented in Table 5-1 show that filters clog and allow only small amounts of smectite particles to pass, and that at a very low rate. The clogging is clearly shown by the comparison with similar experiments with filters with clays without accessory minerals described in Section 5-1. In the experiments with accessory minerals and without flow, erosion stopped after 50–200 days. The highest *initial* erosion flux is about 0.5 kg/m^2/yr. This initial erosion rate cannot be used to assess later rates but the fact that erosion ceases after a short time indicates that the accessory minerals will clog pores (and fractures) 0.1 mm and smaller after a short initial period.

The experiments with flow on the outside and trough filters may be better suited for extrapolation to long times. For the following comparison it may be remembered that in the filter experiments without accessory minerals, Section 5-1, the flux was 20 kg/m^2/yr as assessed by the decrease in swelling pressure. In similar experiments with flow (Figure 5-3) and with accessory minerals the flux was 0.02 and 0.01 kg/m^2/yr respectively. See Figures 5-5 and 5-6. In the nearly 3 year experiment, the largest flux was less than 0.1 kg/m^2/yr initially. It decreased to 0.001 kg/m^2/yr as can be derived from Figure 5-7 for the period spanning 200 to 1 000 days.

For illustration purposes assume that the accessory minerals in the fracture have formed a filter at 5 m distance from the centre of the deposition hole in the fracture with 0.1 mm aperture. The cross section area of this filter is $\pi 2 \times 5 \times 10^{-4}$ m^2 = 0.00314 m^2. With a flux 0.1 kg/m^2/yr the erosion rate would be 3×10^{-4} kg/yr. This value is about four orders of magnitude less than for clays without accessory minerals.

7 Rheologic properties of the eroded montmorillonite from the clay

The largest loss rates are expected in sloping fractures in which flocs formed of the released montmorillonite particles sediment, pulled by gravity. It is described in Neretnieks et al. (2016a) that small flocs can agglomerate to larger flocs that eventually grow large enough to fill out the aperture of the fracture. Then in narrow fractures this agglomerate fluid, AF, will flow downward with a rate determined by its viscosity. In the scoping calculations it was found that unless the viscosity of the AF is more than hundred times larger than that of water the AF can move away as fast as it is released from the source in fractures with apertures that may intersect deposition holes and tunnels. It is well known that natural agglomerates that settle in water and form sediment "age" and can become very viscous. They can even form gel-like structures with yield strength. In the rest of this section we discuss rheological properties of montmorillonite suspensions and especially the properties of sediments that could form of the flocs released in sloping fractures.

The rheological properties of bentonite clay suspensions and purified and homo-ionic montmorillonite suspensions have been extensively studied for industrial applications such as drilling muds. Sediments that contain large amounts of clays in rivers, lakes and seas have also been much investigated and we studied also recent papers in these areas.

Montmorillonite clay properties have lately been studied by Birgersson et al. 2009, 2011), Michot et al. (2004), Paineau et al. (2011), Hedström et al. (2016), Abend and Lagaly (2000), Pujala (2014), Ramos-Tejada et al. (2001), Tsujimoto and Adachi (2011), Tsujimoto et al. (2014), Miyahara et al. (2002), Ali and Bandyopadhyay (2016), Laribi et al. (2005), Au and Leong (2016), Hilhorst et al. (2014), Sakairi et al. (2005) and Bailey et al. (2015). These investigations report rheological data of low ionic strengths, <10 mM, and low solid concentrations, $C_w<6$ % by weight, under different shear rates, down to or less than 0.1 s^{-1}. Low shear rate conditions are of special interest for the present report. There are also numerous other papers in which the main aim has been to study conditions of interest for drilling muds. The general trends are similar although there are sometimes considerable differences that often seem to be related to sample preparation and measurement techniques. There are also often considerable differences between montmorillonites from different sources even when the purification methods are similar. In some cases there also seems to be different influence of ionic strength effects especially in the very lowest ion concentration region. Often comparisons are not facilitated by the way the results are presented. In some papers results are presented mostly in figures of complex elastic and viscous moduli while in other yield stress and/or apparent viscosities are presented. Most investigations seem to be aimed to study shear stress and shear rate regions that are relevant for processes that cover minutes to hours. It is not obvious that these can be extrapolated to the long times of interest for repository conditions. Often details of the measurements are insufficiently reported and may be a reason for the seeming differences between different investigations. Of the large number of paper referred to above we present some details only for those most relevant for our purposes.

Abend and Lagaly (2000) studied the rheological properties of four Na-montmorillonites in suspensions with ion concentrations c_{ion} between, 0.01 and 100 mM. For $C_w = 2$ % suspensions (volume fraction $\phi = 0.75$ %) they found yield strengths decreasing from 1 Pa to about 0.2 Pa when NaCl concentration increased from 0.01 to 1 mM. For two of the montmorillonites it increased to about 10 Pa and for two it remained below 1 Pa when c_{ion} increased to 100 mM. The apparent viscosity μ_a was 3 to 6 times that of water over the entire range of ion concentrations although with a slight dip around 1 mM. Similar results were obtained with K, Cs and Ca instead of Na. Different anions, SO_4^{2-} and $P_2O_7^{4-}$ did not much influence the yield strength τ_y or the apparent viscosity. Increasing C_w up to 5 % increased the τ_y up to 50 Pa. The suspension apparent viscosity decreased with increasing shear rate in this shear-thinning suspension.

Paineau et al. (2011) proposed a model that summarizes their results. One central concept in their model is the equivalent spherical volume fraction ϕ_{sph} proposed by Onsager (1949). This uses the volume of the spheres the particles would sweep by rotation, to define a fictive volume fraction of

sphere-like particles. The idea is that when the suspension is so dilute that the spheres do not touch the suspension behaves like a Newtonian fluid, although more viscous than water. In a more concentrated suspension the spheres interfere with each other and the viscous properties become very different. Liu (2011) successfully used this concept to develop a simple model that fitted a number of different published data for different montmorillonites and ionic strengths for $\phi_{sph} < 1$. For higher concentrations the relation of Paineau et al. (2011) can be used but it is considerably more complex. For the lower actual volume fractions ϕ below around 0.5 %, the viscosity was nearly Newtonian and only slightly increasing with shear rate and age from essentially that of water to 10 to 100 times that of water with increasing ϕ. However, the three montmorillonites investigated differed noticeably.

Bailey et al. (2015) reviewed and summarized the current understanding of smectite phase behaviour and rheology. They present the current view on sol-gel state diagrams, what sometimes is called "phase" behaviour. The term "phase" is not strictly correct in the thermodynamic sense. As in other papers showing similar diagrams there is no indication in the diagrams on floc formation and phase separation in the low ionic strength/low solids region. This region is commonly designated to be sol. Thixotropy is illustrated for cycles of up to 48 minutes but the effect is not large with a maximum difference of shear stress over five cycles of less than a factor of 2. The authors conclude that present models are mainly empirical or at best semi-empirical.

Sakairi et al. (2005) present experimental results on yield stress for a NaMt over an ion concentration range 10^{-5} to 10^{-2} M NaCl and montmorillonite concentration ϕ range of 0.6 to 3 %. The yield stress is highest for the 0.01 mM solution at high volume fractions, about 200 to 300 Pa and lowest for the 10 mM, about 0.1 Pa at the lowest volume fraction of 1.5 % shown in the diagram in the reference. The results suggest that between 1 mM and 5 mM there is a very large change in the rheological behaviour.

Modelling the repulsive force between the smectite sheets by the Gouy-Chapman theory for parallel sheets they found that by assuming the yield stress is equal to the repulsive pressure they could correlate the experimental results reasonably well over the whole range of experimental conditions. There is, however, a need to introduce a correction factor for the Debye length. The factor decreases from 3 to 0.6 when concentration increases from 0.01 mM to 1 mM NaCl.

Laxton and Berg (2006) discuss various approaches of modelling the yield stress as influenced by the z-potential as well by the parallel plate repulsion model mentioned above. They suggest that the face and the edge potential must both be accounted for and find some support in experimental data from Laponite, a well-defined synthetic clay.

Tsujimoto et al. (2014) studied rheology of NaMt at volume fractions 0.02 to 0.2 % in 0.01 to 1 mM NaCl. In this range the suspension viscosity was at most three times larger than water, which agrees well will other measurements.

Tsujimoto and Adachi (2011) made a similar study with NaCl concentration ranging from 5 to 50 mM wherein edge–face interactions between clay sheets are expected to dominate, with similar results except for the highest concentration where the apparent viscosity was clearly larger.

Notwithstanding the differences, there are some clear trends. Very briefly we give an overview of the properties of special importance for the aim of this report. In chemically dilute water c_{ion}, < 10 mM bentonite suspensions with volume fractions below about 0.5–1 % can be characterised as Newtonian fluids with viscosity from that of water at low volume fractions up to ten or more times when approaching ϕ = 0.5–1 %. At higher volume fractions the suspension can become gel-like and exhibit yield stress from a fraction of one Pa to tens to even hundreds of Pa with increasing volume fractions. The elastic gel breaks down when deformed by more than 10 % and becomes fluid with an apparent viscosity that is very high but decreases at higher shear rates. It should also be noted that suspensions with less than 0.5–1 % separate in two "phases" in a gravity field leaving a sediment with more than 0.5–1 % solids and a liquid with very to extremely low concentration of particles. This is of special interest for the aims of the present report because the rheological properties of the phase with the particles will determine the movement of the sediment in the fractures.

Obviously if the suspension has low viscosity and "rapidly" can flow downward in sloping fractures it could travel far. Should the flocculation and gel formation develop near the source the fracture may be clogged by the sediment. Next we present information from various sources that can help to understand and to quantify the processes involved

Sedimentation of dilute suspensions and “phase” separation has attracted attention both from theoretical point of view and for practical application purposes. Studies of a well-defined synthetic clay, Laponite, with similar properties as montmorillonite have been made on rheology, flocculation, sedimentation and aging. Ruzicka et al. (2010) and Angelini et al. (2013) report phase separation at solid concentration above about C_w=1 %. It takes several months to complete the separation. Angelini et al. (2014) also working with Laponite describe self-assembly mechanisms of the particles and show that different coherent structures can result. The term “arrested states” is used to describe the different forms of the structures that can result under different conditions. The term suggests that equilibrium has not been reached but change has been stopped in a local energy minimum pit. Laponite sheets are as thick as those of montmorillonite but about 25 nm in diameter, whereas montmorillonite spans a range from less than 100 to many hundreds of nm. Laponite may not fully reflect the behaviour of montmorillonite but is more well-defined and therefore easier to study. It has been much studied. Michot et al. (2004) found that the size and size distribution of the particles influences the formation and the structures of the agglomerates and the phase diagrams. This adds to the complexities when studying montmorillonite behaviour.

Numerous studies have been made on flocculation, floc sedimentation and rheology of natural sediments in lakes and rivers. A review of the mechanisms of floc strength and breakage can be found in Jarvis et al. (2005). Aging and compaction are important for the development of estuaries in rivers and for shipping. See for example Jeong and Park (2016), Jeong (2014), Kobayashi (2005) and Tambo and Hozumi (1979).

We have only found one study using montmorillonite clay that specifically addresses how rheological properties change over long times. Pujala (2014) studied rheology of Mt that had rested one year and also made observations on phase-separated samples in vials aged up to 4 years. Yield stress and apparent viscosity were considerably larger than in freshly prepared suspensions.

For the further discussion we present a conceptual picture of how and why slurries in general and montmorillonite slurries specifically behave and how they develop over time and with changes in shear rate. We only discuss so low ionic strength conditions that coagulation of particles does not occur by van der Waals forces. Such conditions are said to be below the critical coagulation concentration, CCC, which is about 4–10 mM for mostly sodium-dominated montmorillonites. Above CCC, sufficiently strong gel forms that prohibit release of colloidal particles from the gel under the conditions expected in repository environments.

Less well documented and described is that below 4–10 mM and volume fractions below 1 % due to phase separation also gel forms after weeks to months, although with lower yield strength. The volume fraction of particles in the sediment phase can be very low but still form a coherent structure. This is called empty liquid (Bianchi et al. 2006, Angelini et al. 2013). Under these conditions the thin flat montmorillonite particle faces are negatively and the edges are positively charged and can form complex three-dimensional space-filling agglomerates by face to edge bonds (Hedström et al. 2016). Solid/water mass ratio can be considerably lower than in the CCC coagulated gel but can still be strong enough to support its own weight in water.

It has been observed that colloidal gels that have formed sediment from a suspension at first become increasingly stronger but then suddenly can collapse and loose the yield strength that has been built up. This has been observed and discussed in several papers for different types of colloidal suspensions, none of them containing clays, however. Nevertheless this mechanism could be considered because we have found no papers that systematically have addressed this for montmorillonite suspensions in the low volume fractions of interest here. The collapse mechanism(s) could well be relevant considering the mechanisms described in Poon et al. (1999), Buscall et al. (2009), Teece et al. (2011) and Bartlett et al. (2012). Speculatively, the phenomenon could be envisaged as follows that might be applicable for the phase separating montmorillonites suspension. The sediment formed by weakly attractive colloidal particles forms a space-filling network by the complex face to face, face to edge and edge to edge attraction. The gel compresses slowly under its own weight and forms a gel with yield stress. Over time some weaker bonds are broken and slight rearrangements take place. The volume fraction ϕ in the sediment can initially be well below 1 % and still exhibit a yield stress sufficiently large to support its own weight. Such montmorillonite gels have been stable for many years without collapsing in test tubes and vials in the laboratory (Pujala 2014, Hedström et al. 2016). The height of these gels has been a few cm and a lower limit of the yield strength can thus be estimated from the weight of the gel in water. For a 2 cm high unsupported gel with C_w= 2 %

the density difference to water $\Delta\rho = 20$ kg/m^3. The gel supports its weight $\tau = \Delta\rho g \Delta h = 20 \times 9.81$ 0.02 = 4 Pa. This in the range of reported yield stresses for dilute montmorillonite suspensions at very low shear rates. A taller, 2 m high column, unsupported (no wall friction) would be subject to a stress at the bottom of 400 Pa. This is on the high side of reported values. Even if there is no sudden collapse the gel turns liquid and behaves like a Bingham, body/fluid. Then the viscosity of the fluid will determine the rate of movement.

Chang and Leong (2013) discuss and explore this possibility for Mt clays used as drilling muds. They presents experimental results for $C_w = 7$ % over a wide range of ion concentrations for Li, Na, K and Cs from very low concentrations up to 1 M. These conditions are outside those expected for the interests of the present report but it still may be noted that no collapse of the sediment was found.

In order to explore how the rheological properties of the sediment could be studied in more detail we describe our conceptualisation of the mechanisms involved, some observations, how rheological measurements are made and how these are interpreted. The individual montmorillonite particles released as sol at the clay water interface in the fracture rapidly agglomerate to small flocs. The agglomeration is caused by the edge to face binding by coulombic attraction. The actual meeting of particles is caused by random Brownian diffusion of the particles in stagnant water. It is facilitated and speeded up by the rotation and translation of particles in streamlines with different velocities in water seeping in fractures. The streamlines in the middle of a fracture move much faster than those near the surface and this shear speeds up agglomeration at low flowrates but can tear apart the agglomerates at high flowrates. At very high shear rates $\dot{\gamma} = \frac{du_x}{d_y}$ the flocs disintegrate fully and the sheets align themselves parallel to the streamlines. The viscosity becomes constant and the fluid is Newtonian, at least at reasonably low particle concentrations.

The floc strength, structure and size depend also on the conditions under which they formed. The structure is not uniform and has been observed to be fractal, meaning that it is neither purely two- nor three-dimensional and that it depends on the size of the flocs. These properties have been explored and discussed by Kranenburg (1999) on clay rich sediments in tidal waters and show the complexities in describing flocs and flocculation processes. In chemically reacting systems one can often describe how the system approaches a thermodynamically equilibrium state whatever the starting point of the reaction is. This does not seem to be case for the formation of the three-dimensional structures generated by agglomerations. Different starting conditions lead to different arrested structures each at a stable local energy minimum.

One can conceive a gel, floc and sediment with yield strength to be an elastic solid unless subject to stress larger than the yield strength. It is deformed at lower stress but does not flow. At higher stress it flows. The montmorillonite suspensions are shear thinning which implies that at increasing shear rate the apparent viscosity μ_a, i.e. the ratio of the shear force τ to shear rate, $\mu_a = \tau/\dot{\gamma}$, decreases with increasing $\dot{\gamma}$. Typically a power-law relation is used to describe the relation over a very large range of shear rates. Experiments often cover four orders of magnitude and more. The following equation describes this.

$$\tau = const\ \dot{\gamma}^n \qquad (6\text{-}1)$$

The exponent $0 < n \leq 1$. For n=1 the fluid is Newtonian. An apparent viscosity is sometimes used to denote the same relation

$$\frac{\tau}{\dot{\gamma}} = \mu_a = const\ \dot{\gamma}^{n-1} \qquad (6\text{-}2)$$

Rheological measurements are typically made by subjecting the fluid to imposed shear rate and measuring the shear stress or the opposite i.e. imposing a force (shear stress) and measuring the shear rate. A typical equipment used for clay suspensions is a fixed hollow cylinder in which the fluid is poured and a concentric massive cylinder with slightly smaller diameter that is immersed in the fluid. In the first type of measurement a very low shear rate is imposed by slowly rotating the inner cylinder. The stress on the outer cylinder is monitored until it stabilises. Then the rotation rate is increased stepwise until the entire range of shear rates is covered. The samples are commonly prepared shortly before the measurement and homogenised. This implies that agglomeration has not had time to develop and that the measurement will not detect the properties of aged sediment. Another common type of equipment is the cone and plate rheometer in which a cone rotates with

its tip barely touching the static plate. The fluid that is sheared resides between the cone and plate. The measurement principle is the same. In both types of equipment the mobile part can be made to oscillate with different frequencies and amplitudes instead of rotate. This mode of operation gives better information of when a suspension exhibits elastic properties and when and it turns to a fluid.

One may argue that the results will be conservative for the purpose of predicting how slowly an AF can flow in a fracture, provided the "viscosity" of the range of reasonable shear rates give sufficiently low flowrates. This argument is at present not quite satisfying but could of course be tested by simulations provided appropriate rheological data can be derived. It should, however, be noted that there are considerable uncertainties already in well-performed experiments because different sample preparation techniques can give considerably different results as noted by Birgersson et al. (2009).

The other technique might offer an alternative for aged suspensions, namely imposing a low shear force and measuring the distortion of the sample. If it is ideally elastic it will rapidly yield slightly and then stop deforming. By increasing the force in small steps eventually the sample will "suddenly" yield and become fluid. Then the viscosity measurement stage would begin until the entire range of interest is covered. Also this approach has considerable uncertainties as pointed out by Pujala (2014). However, the structure of an aged gel will not be destroyed initially and at least fairly well defined value of the yield stress could be obtained. There is, however, a concern that this yield stress is not real but that the suspension has a very high viscosity and is subject to so low creep that it is not seen in the measurements, which by necessity are made during a reasonably short time. Although this concern may seem exaggerated we wish to simulate times far in excess of a few years and it should at least be considered how this could be approached.

The few measurements we have found so far in the literature with purified montmorillonite and as received bentonite clays in low ion concentration waters clearly show aging. There also seems to be no drastic differences between clays with and without the naturally present accessory minerals. Nor are there very large differences between essentially deionised water containing samples and samples with concentrations up to 3–4 mM sodium and traces of calcium, which is the range of interest in this report. There is one exception to this (Shalkevich et al. 2007). They found that 1 weight % montmorillonite in 0.01 mM water and 10 mM water behaved essentially in the same way over six order of magnitude shear rate range (10^{-3}–10^{3} s^{-1}). These suspensions behave practically as gels. In contrast at 0.1 mM the fluid was essentially Newtonian. It raises questions about interpreting the results with the unknown montmorillonite concentration in the sediments observed in Schatz and Akhanoba 2016).

When the concentration is below about 2.5 % by weight (about 1 % volume) and structure of the sediment destroyed by some reason, the bonds are broken, and the smectite particles become free to rotate. This suspension (sol) will be a Newtonian fluid (Liu 2011) and will have a viscosity about ten times that of water. Adding external energy can induce such a collapse. It is hardly conceivable that it could be induced by compression by gravity in a fracture in which the sediment is in contact with the fracture surfaces. The friction against the walls counteracts the downward movement of the sediment. Nevertheless it would be valuable to confirm this by experiments with aged sediment actually measuring the stress needed to start the gel movement. This can be compared with model predictions.

8 Discussion and conclusion

The BELBaR project has confirmed and strengthened earlier understanding of smectite behaviour in different waters. The experimental findings that very calcium rich bentonites will not release colloids has been confirmed by theoretic modelling of the behaviour of mono- and divalent ions in the narrow space between smectite sheets (Yang et al. 2016). The formation and properties of very loose smectite flocs has been experimentally shown to be caused by the presence of positively charged edges on the smectite sheets (Hedström et al. 2016). The concept of critical coagulation concentration CCC, as commonly used, has been shown to be oversimplified and potentially considerably misleading. Instead a practical ion concentration range together with information on clay composition, i.e. the ratio of mono- to divalent ions needed to neutralise the permanent negative charge of the smectite was found to well define the condition under which colloid sol can form (Hedström et al. 2016).

Under conditions allowing sol to form, flocculation of the smectite colloids was found to be an important process that strongly influences erosion in stagnant and seeping water in sloping fractures as well as in horizontal fractures with flow (Schatz et al. 2013, Schatz and Akhanoba 2016). Flocculation has been incorporated in the updated model for bentonite expansion and erosion (Neretnieks et al. 2016a).

The released montmorillonite particles form flocs, which in narrow fractures join to become a viscous fluid that is slowed by friction against the fracture walls. It has been reported in the literature that the viscosity of such fluids increases with time. The sedimenting flocs could even form sufficiently strong complex space-filling structures characteristic of gel and develop sufficient yield strength to essentially stop floc movement in fractures. This may considerably decrease the flowrate of the released montmorillonite and possibly even in practice stop further erosion.

In the experiments with clays that contain accessory minerals these are invariably found to clog filters and narrow passages in fractures. This suggests that natural narrow fractures in crystalline rocks will be clogged by the accessory minerals when montmorillonite escapes as colloidal particles leaving the non-colloidal minerals behind. This can effectively decrease the rate of further erosion to negligible levels. The erosion rate becomes several orders of magnitude smaller than earlier predictions in which the presence of accessory minerals is neglected.

The accessory minerals eroded in sloping fractures sediment and collect at the bottom of the fracture unless the sediment can enter the next intersecting fracture. If the slope of the next fracture is smaller than the angle of repose of the sediment it cannot migrate further. The sediment can then build up to the level of the source and stop further clay erosion. This can be especially important for the KBS-3H repository concept.

Considering the large variations in observed erosion rates, no information has been found in the BELBaR investigations or in other relevant literature on montmorillonite suspension properties and behaviour that could seriously increase the erosion rate above that in the model of Neretnieks et al. (2016a). On the contrary, there is a potential that both the gel formation of the eroded clay and the clogging by accessory minerals, even independently, may decrease the erosive loss by several orders of magnitude.

References

SKB's (Svensk Kärnbränslehantering AB) publications can be found at www.skb.com/publications.

Abend S, Lagaly G, 2000. Sol–gel transitions of sodium montmorillonite dispersions. Applied Clay Science 16, 201–227.

Albarran N, Degueldre C, Missana T, Alonso U, García-Gutiérrez M, López T, 2014. Size distribution analysis of colloid generated from compacted bentonite in low ionic strength aqueous solutions. Applied Clay Science 95, 284–293.

Ali S, Bandyopadhyay R, 2016. Effect of electrolytes on the microstructure and yielding of aqueous dispersions of colloidal clay. Soft Matter 12, 414–421.

Angelini R, Ruzicka B, Zaccarelli E, Zulian L, Sztucki M, Moussaïd A, Narayanan T, Sciortino F, 2013. Observation of empty liquids and equilibrium gels in a colloidal clay. AIP Conference Proceedings 1518, 384–390.

Angelini R, Zaccarelli E, de Melo Marques F A, Sztucki M, Fluerasu A, Ruocco G, Ruzicka B, 2014. Glass–glass transition during aging of a colloidal clay. Nature Communications 5. doi.:10.1038/ncomms5049

Apted M, Arthur R, 2012. Initial review of chemical and erosional processes within the buffer and backfill – Geochemical processes. Technical Note 2012:29, Swedish Radiation Safety Authority.

Au P I , Leong Y-K , 2016. Surface chemistry and rheology of slurries of kaolinite and montmorillonite from different sources. KONA Powder and Particle Journal 33, 17–32.

Baik M-H, Cho W-J, Hahn P-S, 2007. Erosion of bentonite particles at the interface of a compacted bentonite and a fractured granite. Engineering Geology 91, 229–239.

Bailey L, Lekkerkerker H N W, Maitland G C, 2015. Smectite clay – inorganic nanoparticle mixed suspensions: phase behaviour and rheology. Soft Matter 11, 222–236.

Bartlett, P, Teece L J, Faers M, 2012. Sudden collapse of a colloidal gel. Physical Review E 85. doi:10.1103/PhysRevE.85.021404

Bianchi E, Largo J, Tartaglia P, Zaccarelli E, Sciortino F, 2006. Phase diagram of patchy colloids: towards empty liquids. Physical Review Letters 97. doi:10.1103/PhysRevLett.97.168301

Birgersson M, Börgesson L, Hedström M, Karnland O, Nilsson U, 2009. Bentonite erosion. Final report. SKB TR-09-34, Svensk Kärnbränslehantering AB.

Birgersson M, Hedström M, Karnland O, 2011. Sol formation ability of Ca/Na-montmorillonite at low ionic strength. Physics and Chemistry of the Earth, Parts A/B/C 36, 1572–1579.

Buscall R, Choudhury T H, Faers M A, Goodwin J W, Luckham P A, Partridge S J, 2009. Towards rationalising collapse times for the delayed sedimentation of weakly-aggregated colloidal gels. Soft Matter 5, 1345.

Chang W-Z, Leong Y-K, 2013. Ageing and collapse of bentonite gels – effects of Li, Na, K and Cs ions. Rheologica Acta 53, 109–122.

Eker O F, Camci F, Jennions I K, 2016. Physics-based prognostic modelling of filter clogging phenomena. Mechanical Systems and Signal Processing 75, 395–412.

Eriksson R, Schatz T, 2015. Rheological properties of clay material at the solid/solution interface formed under quasi-free swelling conditions. Applied Clay Science 108, 12–18.

Guldbrand L, Jönsson B, Wennerström H, Linse P, 1984. Electrical double layer forces. A Monte Carlo study. The Journal of Chemical Physics 80, 2221–2228.

Hedström M, Ekvy Hansen E, Nilsson U, 2016. Montmorillonite phase behaviour. Relevance for buffer erosion in dilute groundwater. SKB TR-15-07, Svensk Kärnbränslehantering AB.

Hilhorst J, Meester V, Groeneveld E, Dhont J K, Lekkerkerker H N, 2014. Structure and rheology of mixed suspensions of montmorillonite and silica nanoparticles. Journal of Physical Chemistry B 118, 11816–11825.

Jansson M, 2009. Bentonite erosion. Laboratory studies. SKB TR-09-33, Svensk Kärnbränslehantering AB.

Jarvis P, Jefferson B, Gregory J, Parsons S A, 2005. A review of floc strength and breakage. Water Research 39, 3121–3137.

Jellander R, Marčelja S, Quirk J P, 1988. Attractive double-layer interactions between calcium clay particles. Journal of Colloid and Interface Science 126, 194–211.

Jeong S W, 2014. The effect of grain size on the viscosity and yield stress of fine-grained sediments. Journal of Mountain Science 11, 31–40.

Jeong S W, Park S-S, 2016. On the viscous resistance of marine sediments for estimating their strength and flow characteristics. Geosciences Journal 20, 149–155.

Jönsson B, Åkesson T, Jönsson B, Meehdi S, Janiak J, Wallenberg R, 2009. Structure and forces in bentonite MX-80. SKB TR-09-06, Svensk Kärnbränslehantering AB.

Kanno T, Wakamatsu H, 1991. Experimental study on bentonite gel migration from a deposition hole. In Proceedings of 3rd International Conference on Nuclear Fuel Reprocessing and Waste Management, RECOD'91, Sendai, Japan, 14–18 April 1991. Tokyo: Atomic Energy Society of Japan, 1005–1010.

Karnland O, Olsson S, Nilsson U, 2006. Mineralogy and sealing properties of various bentonites and smectite-rich clay materials. SKB TR-06-30, Svensk Kärnbränslehantering AB.

Kobayashi M, 2005. Strength of natural soil flocs. Water Research 39, 3273–3278.

Kranenburg C, 1999. Effects of floc strength on viscosity and deposition of cohesive sediment suspensions. Continental Shelf Research 19, 1665–1680.

Laaksoharju M, Smellie J, Tullborg E-L, Gimeno M, Hallbeck L, Molinero J, Waber N, 2008. Bedrock hydrogeochemistry Forsmark. Site descriptive modelling, SDM-Site Forsmark. SKB R-08-47, Svensk Kärnbränslehantering AB.

Laribi S, Fleureau J-M, Grossiord J-L, Kbir-Ariguib N, 2005. Comparative yield stress determination for pure and interstratified smectite clays. Rheologica Acta 44, 262–269.

Laxton P B, Berg J C, 2006. Relating clay yield stress to colloidal parameters. Journal of Colloid and Interface Science 296, 749–755.

Liu L, 2010. Permeability and expansibility of sodium bentonite in dilute solutions. Colloids and Surfaces A: Physicochemical and Engineering Aspects 358, 68–78.

Liu L, 2011. A model for the viscosity of dilute smectite gels. Physics and Chemistry of the Earth, Parts A/B/C 36, 1792–1798.

Liu L, 2013. Prediction of swelling pressures of different types of bentonite in dilute solution. Colloids and Surfaces A: Physicochemical and Engineering Aspects 434, 303–318.

Liu L, Neretnieks I, Moreno L, 2011. Permeability and expansibility of natural bentonite MX-80 in distilled water. Physics and Chemistry of the Earth, Parts A/B/C 36, 1783–1791.

Liu L, Moreno L, Neretnieks I, 2015. Different mechanisms governing the colloidal stability of dispersions of natural bentonite in dilute solutions. BELBaR Deliverable D4.10. European Commission.

Mays D C, Hunt J R, 2007. Hydrodynamic and chemical factors in clogging by montmorillonite in porous media. Environmental Science and Technology 41, 5666–5671.

Michot L J, Bihannic I, Porsch K, Maddi S, Baravian C, Mougel J, Levitz P, 2004. Phase diagrams of Wyoming Na-montmorillonite clay. Influence of particle anisotropy. Langmuir 20, 10829–10837.

Missana T, 2016. Evaluation of experimental results on bentonite erosion. BELBaR Deliverable D2.11. European Commission.

Missana T, Alonso U, Albarran N, García-Gutíerrez M, Cormenzana J-L, 2011. Analysis of colloids erosion from the bentonite barrier of a high level radioactive waste repository and implications in safety assessment. Physics and Chemistry of the Earth, Parts A/B/C 36, 1607–1615.

Missana T, Alonso U, Mayordomo N, Fernandez A M, López T, Hedström M, Ekvy Hansen E, Nilsson U, Bouby M, Heyrich Y, Heck S, Hilpp S, Schäfer T, Liu L, Moreno L, Neretnieks I, Gondolli J, Červinka R, 2016. Final report on experimental results on clay colloid stability WP4. BELBaR Deliverable D4.11, European Commission.

Miyahara K, Adachi Y, Nakaishi K, Ohtsubo M, 2002. Settling velocity of a sodium montmorillonite floc under high ionic strength. Colloids and Surfaces A: Physicochemical and Engineering Aspects 196, 87–91.

Moreno L, Neretnieks I, Liu L, 2010. Modelling of erosion of bentonite gel by gel/sol flow. SKB TR-10-64, Svensk Kärnbränslehantering AB.

Moreno L, Liu L, Neretnieks I, 2011. Erosion of sodium bentonite by flow and colloid diffusion. Physics and Chemistry of the Earth, Parts A/B/C 36, 1600–1606.

Neretnieks I, Liu L, Moreno L, 2009. Mechanisms and models for bentonite erosion. SKB TR-09-35, Svensk Kärnbränslehantering AB.

Neretnieks I, Liu L, Moreno L, 2010. Mass transfer between waste canister and water seeping in rock fractures, Revisiting the Q-equivalent model. SKB TR-10-42, Svensk Kärnbränslehantering AB.

Neretnieks I, Moreno L, Alonso U, Missana T, Schatz T, Červinka R, Sellin P (ed), 2013. Progress report on erosion processes under flowing water conditions. BELBaR Deliverable D2.2. European Commission.

Neretnieks I, Moreno L, Liu L, 2016a. Clay erosion – impact of flocculation and gravitation. SKB TR-16-11, Svensk Kärnbränslehantering AB.

Neretnieks I, Moreno L, Liu L, Olin M, Pulkkanen V-M, Schaefer T, Huber F, Koskinen K (ed), 2016b. Summary of development of conceptual and mathematical models within BELBaR. BELBaR Deliverable D5.3. European Commission.

Onsager L, 1949. The effect of shape on the interaction of colloidal particles. Annals of the New York Academy of Sciences 51, 627–659.

Paineau E, Michot L J, Bihannic I, Baravian C, 2011. Aqueous suspensions of natural swelling clay minerals. 2. Rheological characterization. Langmuir 27, 7806–7819.

Petitjean A, Forquet N, Boutin C, 2016. Oxygen profile and clogging in vertical flow sand filters for on-site wastewater treatment. Journal of Environmental Management 170, 15–20.

Poon W C K, Starrs L, Meeker S P, Moussaïd A, Evans R M L, Pusey P N, Robins M M, 1999. Delayed sedimentation of transient gels in colloid–polymer mixtures: dark-field observation, rheology and dynamic light scattering studies. Faraday Discussions 112, 143–154.

Posiva, 2012. Safety case for the disposal of spent nuclearfuel at Olkiluoto – Design basis. Posiva 2012-3, Posiva Oy, Finland.

Pujala R K, 2014. Dispersion stability, microstructure and phase transition of anisotropic nanodiscs. Cham: Springer International Publishing.

Ramos-Tejada M M, Arroyo F J, Perea R, Dur´n J D G, 2001. Scaling behavior of the rheological properties of montmorillonite suspensions: correlation between interparticle interaction and degree of flocculation. Journal of Colloid and Interface Science 235, 251–259.

Reddi L N, Ming X, Hajra M G, Lee I M, 2000. Permeability reduction of soil filters due to physical clogging. Journal of Geotechnical and Geoenvironmental Engineering 126, 236–246.

Redner S, Datta S, 2000. Clogging time of a filter. Physical Review Letters 84, 6018–6021.

Reid C, Lunn R, El Mountassir G, Tarantino A, 2015. A mechanism for bentonite buffer erosion in a fracture with a naturally varying aperture. Mineralogical Magazine 79, 1485–1494.

Richards T, 2010. Particle clogging in porous media. Filtration of a smectite solution. SKB TR-10-22, Svensk Kärnbränslehantering AB.

Richards T, Neretnieks I, 2010. Filtering of clay colloids in bentonite detritus material. Chemical Engineering & Technology 33, 1303–1310.

Ruzicka B, Zulian L, Zaccarelli E, Angelini R, Sztucki M, Moussaïd A, Ruocco G, 2010. Competing interactions in arrested states of colloidal clays. Physical Review Letters 104. doi:10.1103/PhysRevLett.104.085701

Sakairi N, Kobayashi M, Adachi Y, 2005. Effects of salt concentration on the yield stress of sodium montmorillonite suspension. Journal of Colloid and Interface Science 283, 245–250.

Schatz T, Akhanoba N, 2016. Buffer erosion in sloped fracture environments. Posiva 2016-13, Posiva Oy, Finland.

Schatz T, Kanerva N, Martikainen J, Sane P, Olin M, Seppälä A, Koskinen K, 2013. Buffer erosion in dilute groundwater. Posiva 2012-44, Posiva Oy, Finland.

Shalkevich A, Stradner A, Kumar Bhat S, Muller F, Schurtenberger P, 2007. Cluster, glass, and gel formation and viscoelastic phase separation in aqueous clay suspensions. Langmuir 23, 3570–3580.

SKB, 2011. Long-term safety for the final repository for spent nuclear fuel at Forsmark Main report of the SR-Site project. SKB TR-11-01, Svensk Kärnbränslehantering AB.

Tambo N, Hozumi H, 1979. Physical characteristics of flocs – II. strength of floc. Water Research 13, 421–427.

Teece L J, Faers M A, Bartlett P, 2011. Ageing and collapse in gels with long-range attractions. Soft Matter 7, 1341–1351.

Tsujimoto Y, Adachi Y, 2011. Viscosity of dilute suspensions of weakly flocculated Na-montmorillonite under low pressure gradient. Colloids and Surfaces A: Physicochemical and Engineering Aspects 379, 14–17.

Tsujimoto Y, Kobayashi M, Adachi Y, 2014. Viscosity of dilute Na-montmorillonite suspensions in electrostatically stable condition under low shear stress. Colloids and Surfaces A: Physicochemical and Engineering Aspects 440, 20–26.

Vilks P, Miller N H, 2010. Laboratory bentonite erosion experiments in a synthetic and a natural fracture. NWMO TR-2010-16, Nuclear Waste Management Organization.

Yang G, Liu L, 2015. A systematic comparison of different approaches of density functional theory for the study of electrical double layers. The Journal of Chemical Physics 142, 194110. doi: 10.1063/1.4921376

Yang G, Neretnieks I, Moreno L, Wold S, 2016. Density functional theory of electrolyte solutions in slit-like nanopores II. Applications to forces and ion exchange. Applied Clay Science 132–133, 561–570.

Arkitektkopia AB, Bromma, 2018

SKB is responsible for managing spent nuclear fuel and radioactive waste produced by the Swedish nuclear power plants such that man and the environment are protected in the near and distant future.

skb.se